Electronic Supplementary Information

Double Decker NHC-Cyclometallated Pt Complexes for Highly-Efficient Vacuum-Deposited Green OLEDs and NIR Emission

Irene Melendo,[a] Lucy A. Weatherill,[b] Antonio Martín,[a] Piotr Pander,[c][d] Fernando B. Dias,[b] Sara Fuertes*[a] and Violeta Sicilia*[e]*

CONTENTS **Page**

1. EXPERIMENTAL

1.1. General methods. Compound [{Pt(C^C*)(μ-Cl)}$_2$](**A**) was prepared according to the reported protocol.[1] *N*,*N*′-Diphenylformamidine (N^NH), NEt_3, $AgPF_6$ and $BaSO_4$ were used as purchased from Aldrich, TCI, Fluorochem and Alfa Aesar respectively. IR spectra were recorded on a Perkin-Elmer Spectrum 100 FT-IR Spectrometer (ATR in the range 250-4000 cm^{-1}). Mass spectral analyses were performed with a Microflex MALDI-TOF Bruker or an Autoflex III MALDI-TOF Bruker instruments. C, H, and N analyses were carried out in a Perkin-Elmer 2400 CHNS analyzer. ^{1}H, ^{13}C{^{1}H},^{19}F, ^{195}Pt{^{1}H} NMR spectra were recorded on Bruker Avance 400 MHz instrument using the standard references: $SiMe_4$ for ^{1}H and ^{13}C, $CFCl_3$ for ^{19}F and Na_2PtCl_6 in D_2O for ^{195}Pt. *J* is given in Hz and assignments are based on ^{1}H-^{1}H COSY, ^{1}H-^{13}C HSQC and HMBC experiments.

1.2. X-ray crystallography details

Crystal data and other details of the structure analyses are summarized in Table S1. Single crystals of **2** were obtained by slow diffusion of hexane into saturated solutions of acetone. For **3** and **4-Cl**, they were obtained by slow diffusion of methanol (**3**) and hexane (**4-Cl**) into saturated solutions of dichloromethane. X-ray intensity data were collected at 100 K on a Bruker Apex Duo CCD diffractometer, and the diffraction frames were integrated and corrected for absorption using the SAINT and SADABS software packages.[2] The radiation used in all cases was graphite monochromated MoK_α (λ = 0.71073 Å). The structures were solved with the ShelXT structure solution program using dual methods and refined by full-matrix least squares on F^2 with olex2.refine 1.5[3] (**2** and **4-Cl**) or SHELXL (**3**).[4] All non-hydrogen atoms were assigned anisotropic displacement parameters and refined without positional constraints. All hydrogen atoms were constrained to idealized geometries and assigned isotropic displacement parameters equal

to 1.2 or 1.5 times the U_{iso} values of their attached parent atoms. In the case of **4-Cl**, one of the phenyl residue is disordered over two positions which were refined with 0.5 partial occupancy each. Moreover, there is a great amount of very diffuse solvent (CH_2Cl_2) After some unsuccessful attempts to model these as independent moieties (which led to unacceptable geometrical and displacement anisotropic parameters), a solvent mask was calculated and 470 electrons were found in a volume of 1384 $Å^3$ in 1 void per unit cell (almost 25% of the unit cell volume). This is consistent with the presence of 3[CH_2Cl_2] per formula unit which account for 504 electrons per unit cell. Refinement of these models lead to the parameters listed in Table S1.

CCDC numbers 2515149-2515151 contain the supplementary crystallographic data for the structures reported here.

Table S1: Crystallographic data.

	2	**3**	**4-Cl 3 CH_2Cl_2**
Empirical formula	$C_{40}H_{35}F_6N_6Pt$	$C_{54}H_{44}N_8Pt_2$	$C_{57}H_{50}Cl_8N_8Pt_2$
Formula weight	939.806	1195.15	1520.83
Crystal system	Monoclinic	Monoclinic	Triclinic
Space group	P 2_1/n	C 2/c	P-1
a (Å)	7.629(3)	20.0080(7)	13.652(2)
b (Å)	22.083(6)	16.3673(5)	17.859(5)
c (Å)	21.521(8)	13.2383(4)	24.775(6)
α (º)	90	90	106.249(5)
β (º)	97.715(8)	98.5300(10)	104.523(8)
γ (º)	90	90	95.973(5)
Volume ($Å^3$)/Z	3593.0(2) / 4	4287.3(2) / 4	5514.0(2) / 4
ρ (Mg/m^3)	1.738	1.852	1.832
μ (Mo-Kα) (mm^{-1})	4.020	6.569	5.503
F(000)	1852.9	2320	2960
Crystal size (mm^3)	0.13 x 0.09 x 0.05	0.33 x 0.32 x 0.23	0.35 x 0.21 x 0.09
Theta range (º)	4.16 to 56.60	2.058 to 28.319	4.074 to 56.868
Reflections collected	124786	37687	259708
Independent reflections [R(int)]	8918 [0.0516]	5332 [0.0396]	27554 [0.0755]
Final R_1, wR_2 [I>2sigma(I)][a]	0.0547, 0.1201	0.0171, 0.0379	0.0468, 0.1261
R_1, wR_2 (all data)[a]	0.0586, 0.1221	0.0186, 0.0388	0.0625, 0.1348
Absolute structure parameter	—	—	—
GOF (F^2)[b]	0.976	1.057	1.041
Largest diff. peak and hole/ e.$Å^{-3}$	1.49 and -2.61	1.065 and -0.915	3.20 and -2.05

[a] $R_1 = \sum(|F_o| - |F_c|) / \sum |F_o|$. $wR_2 = [\sum w (F_o^2 - F_c^2)^2 / \sum w(F_o^2)^2]^{1/2}$

[b] Goodness-of-fit = $[\sum w (F_o^2 - F_c^2)^2 / (n_{obs} - n_{param})]^{1/2}$.

1.3. Computational methods. Density functional calculations were carried out on the ground (S_0) and triplet (T_1) state with the Gaussian 16 suite of programs,[5] using the M06 hybrid density functional[6] together with Grimme's D3 dispersion correction.[7] The ECP-60-mwb for Pt and ECP-46-mwb, for I, pseudopotentials[8] were used, and the 6-31G(d)[9, 10] basis sets were used for all other atoms. General geometry optimizations were performed without any symmetry restriction and in the gas phase. Frequency calculations were performed in order to determine the nature of the stationary points found in S_0 and T_1 (no imaginary frequencies for minima). The time-dependent density-functional (TD-DFT) calculations were carried out in the gas phase. ChemissianLab program package was used for analysis and graphic representation of molecular orbitals and for Mayer Bond Order analysis. Atomic coordinates for the optimized structures are included as a separate .xyz file.

1.4. Photophysical methods. UV-visible spectra in solution were registered on a JASCO V-780 spectrophotometer. The photoluminescence experiments were carried out in quartz tubes under argon atmosphere. Steady-state photoluminescence spectra were recorded on in a FluoTime 300 spectrofluorometer (PicoQuant GmbH) equipped with a NIR-PMT detector (Hamamatsu H10330C-75) using a 300 W Xenon lamp or a Fluorolog spectrometer with a Xenon lamp excitation source. Emission lifetime measurements were recorded with Picosecond Laser Diodes (371, 450 nm) or a pulse Xe lamp, as excitation sources and using the EasyTau II software package (PicoQuant GmbH). Data analysis was performed using the built-in software FluoFit (PicoQuant GmbH). Time resolved photoluminescence decays were measured by detecting emission on a gated iCCD camera (Stanford Computer Optics) with a sub-nanosecond resolution. Excitation was provided by the third harmonic of a pulsed Nd:YAG laser (355 nm). Quantum yields were measured using the Hamamatsu Absolute PL Quantum Yield Measurement System

C11347-11 at room temperature. PMMA films were prepared by dissolving the Pt complexes in 1 mL of dichloromethane ($5 \cdot 10^{-4}$ M **2** due to solubility issues and 10^{-2} M **3**). After that, PMMA (98 % weight) was slowly added with vigorous stirring. The solutions were deposited on optical grade quartz plates of 1x1 cm by drop casting, and allowed to dry overnight before the measurements were carried out.

1.5. Electrochemical methods. Cyclic voltammetry of **3** was performed using a PalmSens*4* electrochemistry workstation in a 25 x 40 mm three-electrode electrochemical cell equipped with glassy carbon working electrode (BASi, 3 mm diameter), an Ag/AgCl (3 M KCl) electrode reference (BASi), and a platinum wire auxiliary electrode (BASi, 7.5 cm x 0.5 mm diameter). All experiments were performed at 298 K under an argon atmosphere, using a degassed $5x10^{-4}$ M solution in CH_2Cl_2 containing 0.1 M NBu_4PF_6 as the supporting electrolyte. Measurements were conducted with scan rates of 50, 100, 250, 300 and 500 mV/s, and ferrocenium/ferrocene (Fc+/Fc) was used as the internal standard.

1.6. OLEDs fabrication. Devices were fabricated on glass substrates coated with indium tin oxide (ITO) with a sheet resistance of 20 Ω/sq and 100 nm thickness of ITO. Substrates were washed with distilled water followed by acetone and then sonicated in acetone and isopropanol, for 15 minutes each. Substrates were dried with compressed air and placed into an oxygen plasma generator for 6 minutes. Layers were thermally deposited at a pressure of 10^{-6} mbar using a Kurt J. Lesker Spectros II deposition system. Deposition rates between 0.05 and 3.1 $Å s^{-1}$ were used depending on the thickness of the layer. Each device comprised four pixels of varying sizes 4x4, 4x2 or 2x2 mm. The characterisation of devices was done using a 10-inch integrating sphere (Labsphere) connected to a Source Measure Unit (SMU, Keithley) and a QePro spectrometer (OceanOptics).

1.7. Synthesis of new compounds.

[Pt(C^C*)(NCMe)$_2$]PF$_6$ (1). $AgPF_6$ (159.6 mg, 0.63 mmol) was added to a yellow suspension of **A** (300.0 mg, 0.31 mmol) in acetonitrile (80 mL) at RT. After 8 h stirring, the resulting mixture was filtered through Celite and evaporated to dryness. Addition of diethyl ether (2x10 mL) to the residue rendered **1** as a pure yellow solid. Yield: 364.8 mg (92%). Anal. Calcd. for $C_{18}H_{17}N_4F_6PPt$: C, 34.35; H, 2.72; N, 8.90. Found: C, 34.02; H, 2.58; N; 8.79. ^{1}H NMR data (300 MHz, CD_3CN): 7.84 (s, $^3J_{H\text{-}Pt}$ = 66.8, 1H, H_{naph} C^C*); [7.83-7.75] (m, 2H, H_{naph} C^C*); 7.65 (d, $^4J_{H\text{-}Pt}$ = 8.9, $^3J_{H\text{-}H}$ = 2.1, 1H, H_{im} C^C*); 7.62 (s, $^3J_{H\text{-}Pt}$ = 16.5, 1H, H_{naph} C^C*); [7.46-7.41] (m, 2H, H_{naph} C^C*); 7.16 (d, $^4J_{H\text{-}Pt}$ = 12.4, $^3J_{H\text{-}H}$ = 2.1, 1H, H_{im} C^C*); 3.83 (s, CH_3 C^C*); 1.96 (s, 6H, MeCN). IR (cm^{-1}): 833, 556 (PF_6).

[Pt(C^C*)(N^NH)$_2$]PF$_6$ (2). *N*,*N*′-Diphenylformamidine (202.1 mg, 1.03 mmol) was added to a suspension of **1** (161.3 mg, 0.26 mmol) in methanol (30 mL) at r.t in the dark. After 3 h stirring, the resulting mixture was concentrated to *ca.* 1 mL. Addition of diethylether (15 mL) to the residue rendered a white solid, that was filtered and washed with diethylether (2 x 5 mL) to give **2** as a white solid. Yield: 173.6 mg (72%). Anal. Calcd. for $C_{40}H_{35}F_6N_6PPt$: C, 51.12; H, 3.75; N, 8.94. Found: C, 50.91; H, 3.76; N, 8.91. ^{1}H NMR data (400 MHz, CD_2Cl_2): δ = [8.32-8.19] (m, 4H, 2 NC*H*N, 2 N*H*); 7.82 (d, $^3J_{H\text{-}H}$ = 8.0, 1H, H_{naph} C^C*); 7.71 (s, 1H, H_{naph} C^C*); 7.69 (d, $^3J_{H\text{-}H}$ = 2.1, 1H, H_{im} C^C*); [7.65-7.61] (m, 2H, H_{naph} C^C*); [7.52-7.13] (m, 19H, 2H_{naph} C^C*, H_{im} C^C*, 16 H_{Ph} N^N); [6.81-6.72] (m, 4H, H_{Ph} N^N); 3.82 (s, 3H, CH_3 C^C*). ^{13}C{^{1}H} NMR plus HMBC and HSQC (100.6 MHz, CD_2Cl_2): δ = 153.6 (s, C_{NHC} C^C*); 152.5 and 152.4 (s, NC*H*N); 147.9 and 147.8 (s, C_{Ph} N^N); 134.5 (s, C_{naph} C^C*); 132.3 (s, C_{naph} C^C*); 130.5, 130.4, 130.3 and 130.2 (s, C_{Ar}); 127.9 (s, C_{naph} C^C*); 127.6 (s, C_{naph} C^C*); 127.5, 126.5, 126.4, 126.3 and 126.2 (s, C_{Ar}); 124.0 (s, C_{im} C^C*); 123.5, 122.8, 119.2 and 119.0 (s, C_{Ar}); 115.8

(s, C_{im} C^C*); 108.8 (s, C_{naph} C^C*); 36.6 (s, CH_3 C^C*). $^{195}Pt\{^1H\}$ NMR (85.6 MHz, CD_2Cl_2): δ = – 3936.1 (s). MS (MALDI+): *m/z* IR (cm^{-1}): 556, 833 (PF_6)

[{Pt(C^C*)(*μ*-N^N)}$_2$] (3). 1 mL of NEt_3 was added to a suspension of **2** (171.2 mg, 0.18 mmol) in 2-methoxyethanol (8 mL). After stirring at reflux in the dark for 2h, the resulting mixture was evaporated to dryness. Addition of methanol (5 mL) to the residue rendered a dark yellow solid, that was filtered and washed with methanol (2 x 2 mL) to give **3**. Yield: 83.3 mg (77%). Anal. Calcd. for $C_{54}H_{44}N_8Pt_2$: C, 54.27; H, 3.71; N, 9.38. Found: C, 53.81; H, 3.54; N, 9.08. ^1H NMR data (400 MHz, CD_2Cl_2): δ = 8.52 (s, 2H, NC*H*N); 7.76 (s, 2H, H_{naph} C^C*); 7.64 (d, $^3J_{H-H}$ = 7.8, 2H, H_{naph} C^C*); [7.60-7.56] (m, 6H, 2H_{naph}, 4H_{Ph} N^N); 7.43 (d, $^3J_{H-H}$ = 7.8, 4H, H_{Ph} N^N); [7.32-7.20] (m, 8H, 4H_{naph} C^C*, 4H_{Ph} N^N); 7.08 (s, 2H, H_{naph} C^C*); 7.05 (t, $^3J_{H-H}$ = 7.6, 4H, H_{Ph} N^N); 6.98 (t, $^3J_{H-H}$ = 7.4, 2H, H_{Ph} N^N); 6.89 (d, $^3J_{H-H}$ = 2.0, 2H, H_{im} C^C*); 6.84 (d, $^3J_{H-H}$ = 7.3, 2H, H_{Ph} N^N); 5.91 (d, $^3J_{H-H}$ = 2.0, 2H, H_{im} C^C*); 2.32 (s, 6H, CH_3 C^C*). $^{13}C\{^1H\}$ NMR plus HMBC and HSQC (100.6 MHz, CD_2Cl_2): δ = 160.8 (s, NC*H*N); 158.8 (s, C_{NHC} C^C*); 153.4 (s, C_{Ph} N^N); 152.3 (s, C_{Ph} N^N); 147.0 (s, C_{naph} C^C*); 133.3 (s, C_{naph} C^C*); 132.8 (s, C_{naph} C^C*); 131.5 (s, C_{naph} C^C*); 131.2 (s, C_{naph} C^C*); 128.8 (s, C_{Ph} N^N); 128.5 (s, C_{Ph} N^N); 127.3 (s, C_{naph} C^C*); 126.8 (s, C_{naph} C^C*); 124.8 (s, C_{naph} C^C*); 124.6 (s, C_{Ph} N^N); 124.1 (s, C_{naph} C^C*); 123.5 (s, C_{Ph} N^N); 123.2 (s, C_{Ph} N^N); 122.5 (s, C_{Ph} N^N); 121.3 (s, C_{im} C^C*); 113.2 (s, C_{im} C^C*); 106.1 (s, C_{naph} C^C*); 35.5 (s, CH_3 C^C*). $^{195}Pt\{^1H\}$ NMR (85.6 MHz, CD_2Cl_2): δ = – 3524.3 (s). MS (MALDI+): *m/z* 1194.1 [{Pt(C^C*)(*μ*-N^N)}$_2$]

[{Pt(C^C*)(*μ*-N^N)Cl}$_2$] (4-Cl). Method A: A solution of compound **3** (80.0 mg, 0.07 mmol) in $CHCl_3$ (20 mL) was left to react in the air, at RT and irradiating with 365 nm UV light. After 1.5 h of reaction, the mixture was concentrated to *ca.* 1 mL and treated with *n*-hexane (20 mL); the resulting precipitate was filtered, washed with *n*-hexane (2 x

5 mL), and dried. The solid was recrystallized by redissolving in 2 mL of CH_2Cl_2 and precipitated with 30 mL of diethylether. The suspension was then filtered, washed and dried to give **4-Cl** as a brown-orange solid. Yield: 35.8 mg (42%)**. Method B:** $PhICl_2$ (23.2 mg, 0.08 mmol) was added to a suspension of **3** (100.6 mg, 0.08 mmol) in acetone (40 mL) in the air, at RT. After 3 h, the solution was concentrated to *ca.* 3 mL and then 20 mL of *n*-hexane was added to give an orange solid that was filtered, washed, and dried. Yield: 81.6 mg (77%). Anal. Calcd. for $C_{54}H_{44}Cl_2N_8Pt_2$: C, 51.23; H, 3.50; N, 8.85. Found: C, 50.67; H, 3.19; N, 8.10. ^{1}H NMR data (400 MHz, CD_2Cl_2): δ = 8.49 (s, $^3J_{H\text{-}Pt}$ = 76.6, $^3J_{H\text{-}Pt}$ = 60.1, 2H, NC*H*N); 8.19 (s, $^3J_{H\text{-}Pt}$ = 38.4, 2H, H_{naph} C^C*); 7.90 (d, $^3J_{H\text{-}H}$ = 8.1, 2H, H_{naph} C^C*); 7.70 (d, $^3J_{H\text{-}H}$ = 8.1, 2H, H_{naph} C^C*); [7.55-7.46] (m, 6H, 2H_{naph} C^C*, 4H_{Ph} N^N); 7.40 (m, 2H, H_{naph} C^C*); 7.34 (t, $^3J_{H\text{-}H}$ = 7.6, 4H, H_{Ph} N^N); 7.23 (t, $^3J_{H\text{-}H}$ = 7.4, 2H, H_{Ph} N^N); 7.18 (s, $^4J_{H\text{-}Pt}$ = 7.2, 2H, H_{naph} C^C*); 7.07 (d, $^3J_{H\text{-}H}$ = 2.0, 2H, H_{im} C^C*); 7.00 (t, $^3J_{H\text{-}H}$ = 7.3, 4H, H_{Ph} N^N); 6.90 (t, $^3J_{H\text{-}H}$ = 7.2, 2H, H_{Ph} N^N); 6.84 (d, $^3J_{H\text{-}H}$ = 7.3, 4H, H_{Ph} N^N); 5.95 (d, $^3J_{H\text{-}H}$ = 2.0, 2H, H_{im} C^C*); 2.35 (s, 6H, CH_3). ^{13}C{^{1}H} NMR plus HMBC and HSQC (100.6 MHz, CD_2Cl_2): δ = 168.2 (s, NC*H*N); 150.8 (s, C_{Ph} N^N); 149.7 (s, C_{Ph} N^N); 144.8 (s, C_{NHC} C^C*); 141.9 (s, C_{naph} C^C*); 132.7 (s, C_{naph} C^C*); 131.4 (s, C_{naph} C^C*); 131.2 (s, C_{naph} C^C*); 129.5 (s, C_{Ph} N^N); 128.1 (s, C_{Ph} N^N); 127.9 (s, C_{Ph} N^N); 127.4 (s, C_{Ph} N^N); 127.3 (s, C_{naph} C^C*); 126.1 (s, C_{Ph} N^N); 126.0 (s, C_{naph} C^C*); 124.3 (s, C_{Ph} N^N); 123.8 (s, C_{im} C^C*); 120.1 (s, C_{naph} C^C*); 113.7 (s, C_{im} C^C*); 108.7 (s, $^3J_{C\text{-}Pt}$ = 20.3, C_{naph} C^C*); 37.0 (s, CH_3). ^{195}Pt{^{1}H} NMR (85.6 MHz, CD_2Cl_2): δ = – 2313.0 (s). MS (MALDI+): *m/z* 1229.5 [{Pt(C^C*)(μ-N^N)}$_2$Cl], 1193.6 [{Pt(C^C*)(μ-N^N)}$_2$]

[{Pt(C^C*)(μ-N^N)Br}$_2$] (4-Br). $CHBr_3$ (0.1 mL, 1.14 mmol) was added to a suspension of **3** (83.3 mg, 0.07 mmol) in acetone (30 mL) in the air, at RT, and irradiating with 365 nm UV light. After 30 min, the solution was concentrated to *ca.* 2 mL and then

20 mL of *n*-hexane was added to give a brown solid that was filtered, washed with methanol (2 x 2 mL), and dried. Yield: 51.3 mg (54%). Anal. Calcd. for $C_{54}H_{44}Br_2N_8Pt_2$: C, 47.87; H, 3.27; N, 8.27. Found: C, 47.14; H, 3.09; N, 7.60. ^{1}H NMR data (400 MHz, CD_2Cl_2): δ = 8.54 (s, $^3J_{H\text{-}Pt}$ = 76.8, $^3J_{H\text{-}Pt}$ = 60.0, 2H, NC*H*N); 8.22 (s, $^3J_{H\text{-}Pt}$ = 38.8, 2H, H_{naph} C^C*); 7.93 (d, $^3J_{H\text{-}H}$ = 8.0, 2H, H_{naph} C^C*); 7.76 (d, $^3J_{H\text{-}H}$ = 8.0, 2H, H_{naph} C^C*); [7.57-7.49] (m, 6H, 2H_{naph} C^C*, 4H_{Ph} N^N); 7.43 (m, 2H, H_{naph} C^C*); 7.34 (t, $^3J_{H\text{-}H}$ = 7.6, 4H, H_{Ph} N^N); [7.26-7.21] (m, 4H, 2H_{naph} C^C*, 2H_{Ph} N^N); 7.15 (d, $^3J_{H\text{-}H}$ = 2.0, 2H, H_{im} C^C*); 7.00 (m, 4H, H_{Ph} N^N); 6.90 (m, 2H, H_{Ph} N^N); 6.83 (d, $^3J_{H\text{-}H}$ = 7.6, 4H, H_{Ph} N^N); 6.05 (d, $^3J_{H\text{-}H}$ = 2.0, 2H, H_{im} C^C*); 2.35 (s, 6H, CH_3). ^{13}C{^{1}H} NMR plus HMBC and HSQC (100.6 MHz, CD_2Cl_2): δ = 168.0 (s, NC*H*N); 150.8 (s, C_{Ph} N^N); 150.1 (s, C_{Ph} N^N); 143.8 (s, C_{NHC} C^C*); 142.0 (s, C_{naph} C^C*); 132.8 (s, C_{naph} C^C*); 131.5 (s, C_{naph} C^C*); 131.1 (s, C_{naph} C^C*); 129.6 (s, C_{Ph} N^N); 128.4 (s, C_{Ph} N^N); 128.1 (s, C_{Ph} N^N); 127.4 and 127.3 (s, C_{naph} C^C*); 127.2 (s, C_{Ph} N^N); 126.2 (s, C_{Ph} N^N); 126.1 and 126.0 (s, C_{naph} C^C*); 124.6 (s, C_{Ph} N^N); 123.9 (s, C_{im} C^C*); 113.7 (s, C_{im} C^C*); 108.7 (s, C_{naph} C^C*); 37.2 (s, CH_3). ^{195}Pt{^{1}H} NMR (85.6 MHz, CD_2Cl_2): δ = – 2458.8 (s). MS (MALDI+): *m/z* 1194.1 [{Pt(C^C*)(*μ*-N^N)}$_2$]

[{Pt(C^C*)(*μ*-N^N)I}$_2$] (4-I). CHI_3 (79.8 mg, 0.20 mmol) was added to a suspension of **3** (78.6 mg, 0.07 mmol) in acetone (30 mL) in the air, at RT, and irradiating with 365 nm UV-light. After 30 min, the solution was concentrated to *ca.* 2 mL and then 20 mL of *n*-hexane was added to give a red garnet solid that was filtered, washed, and dried. Yield: 68.0 mg (71%). Anal. Calcd. for $C_{54}H_{44}I_2N_8Pt_2$: C, 44.76; H, 3.06; N, 7.73. Found: C, 44.26; H, 3.06; N, 7.08. ^{1}H NMR data (400 MHz, CD_2Cl_2): δ = 8.65 (s, $^3J_{H\text{-}Pt}$ = 76.2, $^3J_{H\text{-}Pt}$ = 58.5, 2H, NC*H*N); 8.24 (s, $^3J_{H\text{-}Pt}$ = 39.8, 2H, H_{naph} C^C*); 7.93 (d, $^3J_{H\text{-}H}$ = 8.3, 2H, H_{naph} C^C*); 7.77 (d, $^3J_{H\text{-}H}$ = 8.3, 2H, H_{naph} C^C*); [7.61-7.51] (m, 6H, 2H_{naph} C^C*, 4H_{Ph} N^N); [7.45-7.32] (m, 6H, 2H_{naph} C^C*, 4H_{Ph} N^N); [7.28-7.22] (m, 4H, 2H_{naph} C^C*, 2H_{Ph} N^N);

7.17 (d, $^3J_{H\text{-}H}$ = 1.8, 2H, H_{im} C^C*); [7.05-6.98] (m, 4H, H_{Ph} N^N); [6.95-6.86] (m, 6H, H_{Ph} N^N); 6.06 (d, $^3J_{H\text{-}H}$ = 1.9, 2H, H_{im} C^C*); 2.27 (s, 6H, CH_3). $^{13}C\{^1H\}$ NMR plus HMBC and HSQC (100.6 MHz, CD_2Cl_2): δ = 167.4 (s, N*C*HN); 151.1 and 151.0 (s, C_{Ph} N^N); 142.3 (s, C_{NHC} C^C*); 132.8 (s, C_{naph} C^C*); 131.5 (s, C_{naph} C^C*); 131.0 (s, C_{naph} C^C*); 129.6 (s, C_{Ph} N^N); 129.1 (s, C_{Ph} N^N); 128.2 (s, C_{Ph} N^N); 127.3 (s, C_{naph} C^C*); 127.3 (s, C_{naph} C^C*); 127.1 (s, C_{Ph} N^N); 126.3 (s, C_{Ph} N^N); 126.0 (s, C_{naph} C^C*); 125.9 (s, C_{naph} C^C*); 124.8 (s, C_{Ph} N^N); 123.9 (s, C_{im} C^C*); 113.6 (s, C_{im} C^C*); 108.6 (s, C_{naph} C^C*); 37.7 (s, CH_3). $^{195}Pt\{^1H\}$ NMR (85.6 MHz, CD_2Cl_2): δ = – 2697.8 (s). MS (MALDI+): *m/z* 1193.7 [{Pt(C^C*)(*μ*-N^N)}$_2$]

Preparation of [(C^C*)Pt(*μ*-(N^N)$_2$Pt(C^C*)(CH$_3$)]BF$_4$ (5). Me_3OBF_4 (25.0 mg, 0.16 mmol) was added to a suspension of **3** (97.3 mg, 0.08 mmol) in anhydrous dichloromethane (15 mL) and the resulting solution was stirred at RT under Ar atmosphere, in the dark for 3 h. Then, the solution was concentrated to *ca.* 1 mL and treated with diethylether (15 mL). The suspension was filtered and washed with diethylether (2 x 5 mL), obtaining a solid that was recrystallized in CH_2Cl_2/Et_2O (1/15 mL) to give **5** as an orange solid. Yield: 59.7 mg (57%). Anal. Calcd for $C_{55}H_{47}BF_4N_8Pt_2$: C, 50.93; H, 3.65; N, 8.64. Found: C, 49.44; H, 3.45; N, 8.44. ^1H NMR data (300 MHz, CD_2Cl_2): δ = 8.69 (s, $^3J_{H\text{-}Pt}$ = 83.9, $^3J_{H\text{-}Pt}$ = 40.5, 1H, NC*H*N); 8.49 (s, $^3J_{H\text{-}Pt}$ = 59.3, 1H, NC*H*N); 8.09 (s, $^3J_{H\text{-}Pt}$ = 42.3, 1H, H_{naph} C^C* [Pt-CH_3]); [7.92-7.78] (m, 4H, 3H_{naph} C^C*, H_{naph} C^C* [Pt]); [7.76-7.71] (m, 1H, H_{naph} C^C*); [7.57-7.54] (m, 2H, H_{naph} C^C* [Pt-CH_3], H_{im} C^C* [Pt-CH_3]); [7.57-7.54] (m, 8H, H_{naph} C^C* [Pt], H_{im} C^C* [Pt], 4H_{naph} C^C*, 2H_{Ph} N^N); [7.40-7.35] (m, 3H, H_{Ph} N^N); [7.28-7.16] (m, 7H, H_{Ph} N^N); [7.14-7.10] (m, 2H, H_{Ph} N^N); [7.06-7.03] (m, 3H, H_{Ph} N^N); [6.94-6.87] (m, 1H, H_{Ph} N^N); [6.61-6.55] (m, 2H, H_{Ph} N^N); 6.14 (d, $^3J_{H\text{-}H}$ = 2.1, 1H, H_{im} C^C* [Pt-CH_3]); 6.00 (d, $^3J_{H\text{-}H}$ = 2.1, 1H, H_{im} C^C* [Pt]); 2.84 (s, 3H, CH_3 C^C* [Pt-CH_3]); 2.24 (s, 3H, CH_3 C^C* [Pt]); 1.64 (s, $^2J_{H\text{-}Pt}$ =

65.7, $^{3}J_{H\text{-}Pt}$ = 15.6, 3H, Pt-*CH*$_3$). $^{13}C\{^{1}H\}$ NMR plus HMBC and HSQC (100.6 MHz, CD_2Cl_2): δ = 164.5 (s, $^{2}J_{C\text{-}Pt}$ = 20.9, N*C*HN); 162.7 (s, N*C*HN); 154.5 (s, C_{NHC} C^C* [Pt]); 150.9 (s, C_{Ph} N^N); 150.0 (s, C_{Ph} N^N); 148.3 (s, C_{Ph} N^N); 147.2 (s, C_{Ph} N^N); 145.1 (s, C_{naph} C^C*); 142.6 (s, C_{NHC} C^C* [Pt-CH_3]); 140.7 (s, C_{naph} C^C*); 134.6 (s, $^{2}J_{C\text{-}Pt}$ = 26.5, C_{naph} C^C* [Pt]); 132.9, 132.4, 132.2 and 132.1 (s, C_{naph} C^C*); 131.9 (s, C_{naph} C^C* [Pt-CH_3]); 129.8, 129.6, 129.5 and 129.0 (s, C_{Ph} N^N); 128.4 (s, C_{naph} C^C*);128.2 (s, C_{Ph} N^N); 127.3 and 127.2 (s, C_{naph} C^C*); 127.0, 126.9, 126.8, 126.6 and 126.4 (s, C_{Ph} N^N, C_{naph} C^C*); 125.8 (s, C_{Ph} N^N); 125.4 (s, C_{Ph} N^N); 125.1 (s, C_{im} C^C* [Pt-CH_3]); 123.9 (s, C_{Ph} N^N); 123.8 (s, C_{im} C^C* [Pt]); 123.1 (s, C_{Ph} N^N); 117.0 (s, C_{im} C^C* [Pt-CH_3]); 115.9 (s, C_{im} C^C* [Pt]); 115.5 (s, $^{3}J_{C\text{-}Pt}$ = 22.7, C_{naph} C^C* [Pt-CH_3]); 109.7 (s, $^{3}J_{C\text{-}Pt}$ = 24.7, C_{naph} C^C* [Pt]); 37.2 (s, CH_3 C^C* [Pt-CH_3]); 36.3 (s, CH_3 C^C* [Pt]); 10.2 (s, $^{1}J_{C\text{-}Pt}$ = 521.7, $^{2}J_{C\text{-}Pt}$ = 153.6, 3H, Pt-*CH*$_3$). $^{195}Pt\{^{1}H\}$ NMR (85.6 MHz, CD_2Cl_2): δ = – 2373.4 (s, $^{1}J_{Pt,\,Pt}$ = 2155.4), – 3264.1. MS (ESI+): *m/z* 1210.32 $[M]^+$.

2. NMR STUDIES FOR CHARACTERIZATION

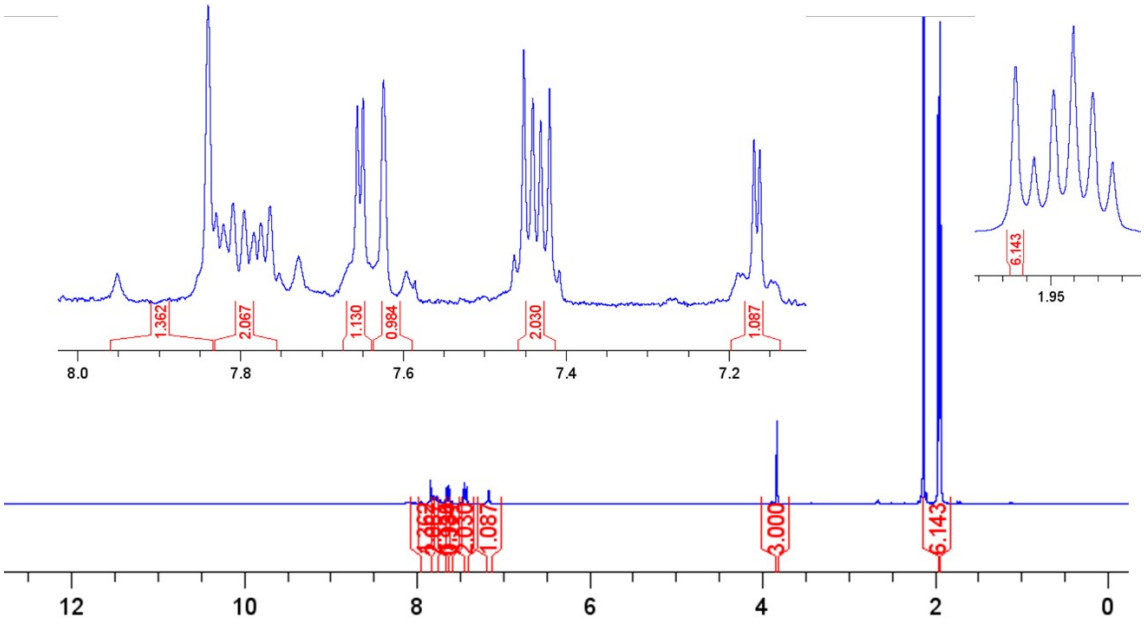

(a)

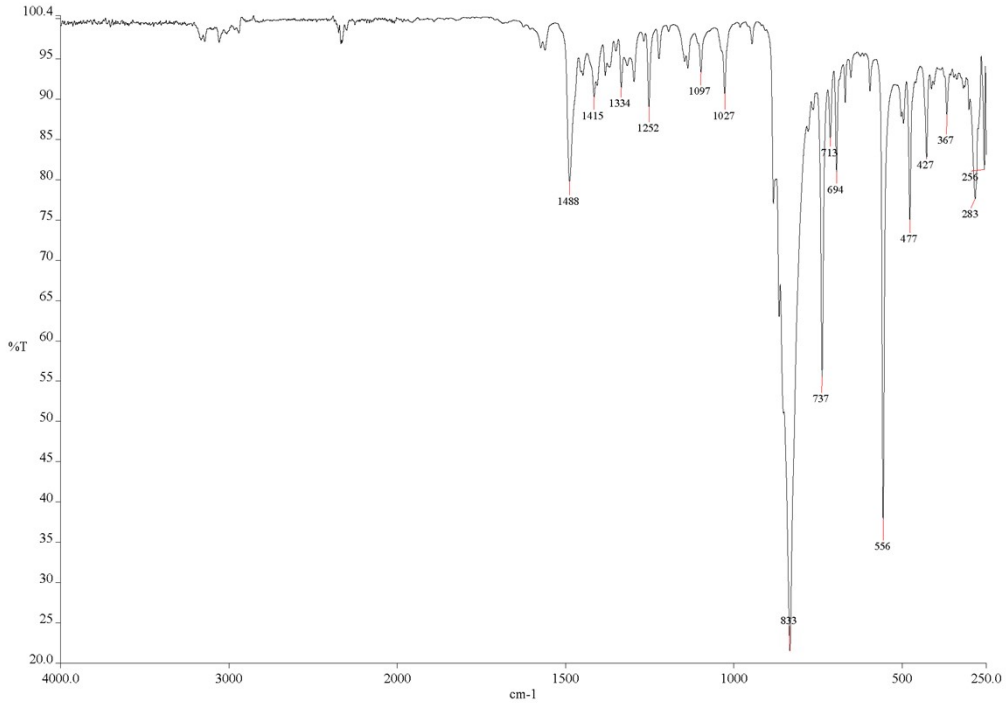

(b)

Figure S1. a) ^{1}H NMR spectrum of **1** in MeCN-d_3; b) IR spectrum of **1**

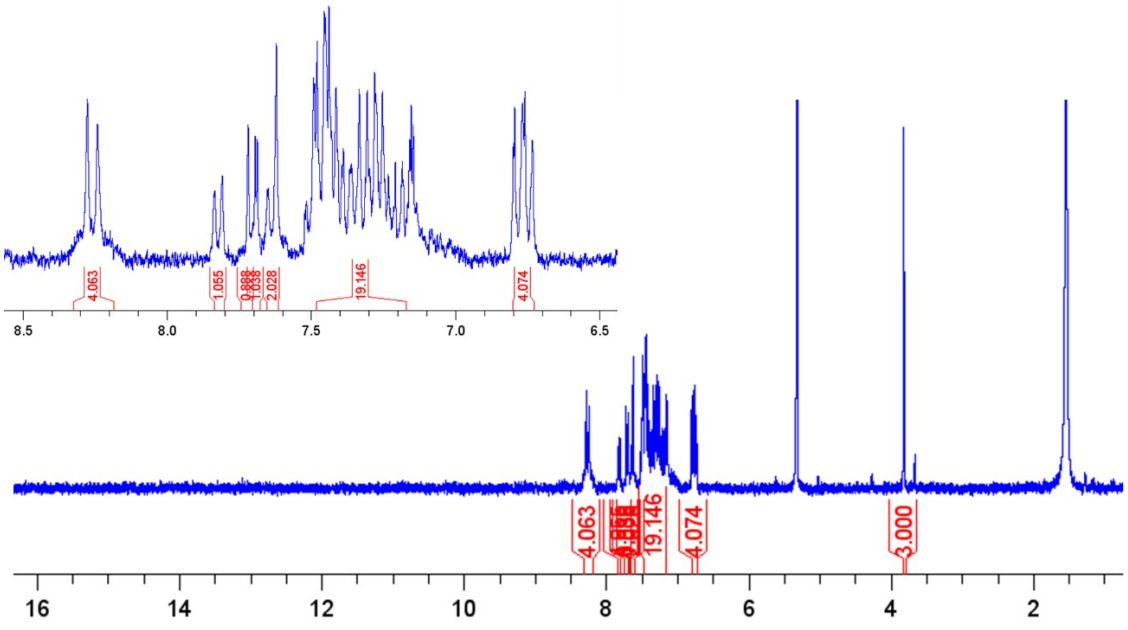
4.063
1.055
0.888
1.038
2.028
19.146
4.074
8.5
8.0
7.5
7.0
6.5
4.063
19.146
4.074
3.000
16
14
12
10
8
6
4
2

(a)

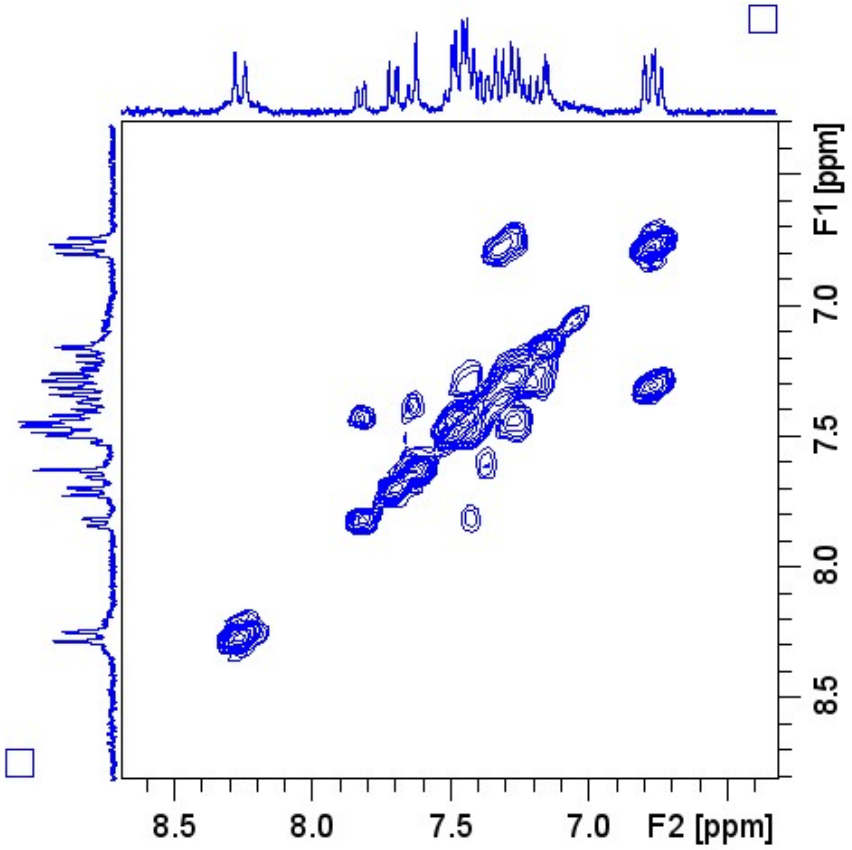
F1 [ppm]
7.0
7.5
8.0
8.5
8.5
8.0
7.5
7.0
F2 [ppm]

(b)

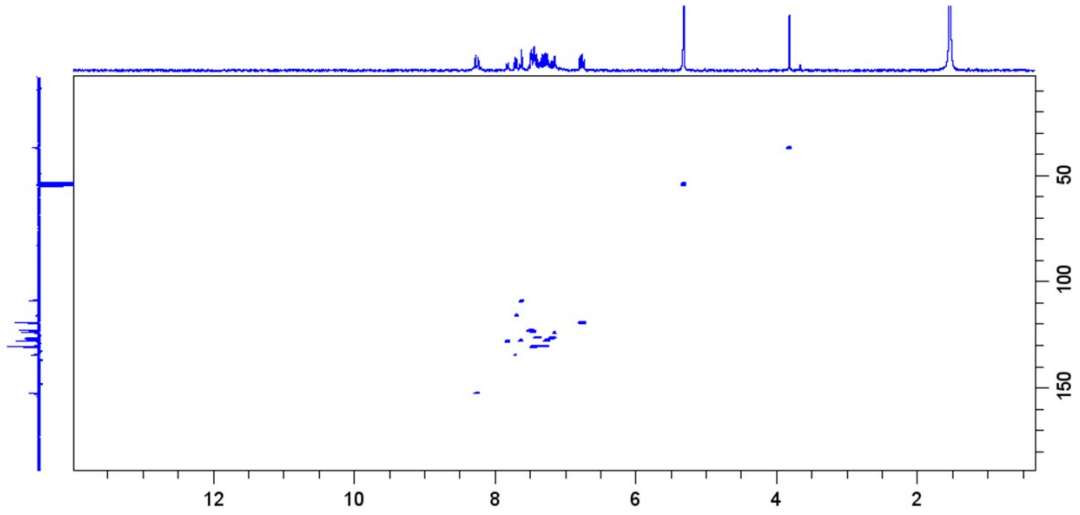

(c)

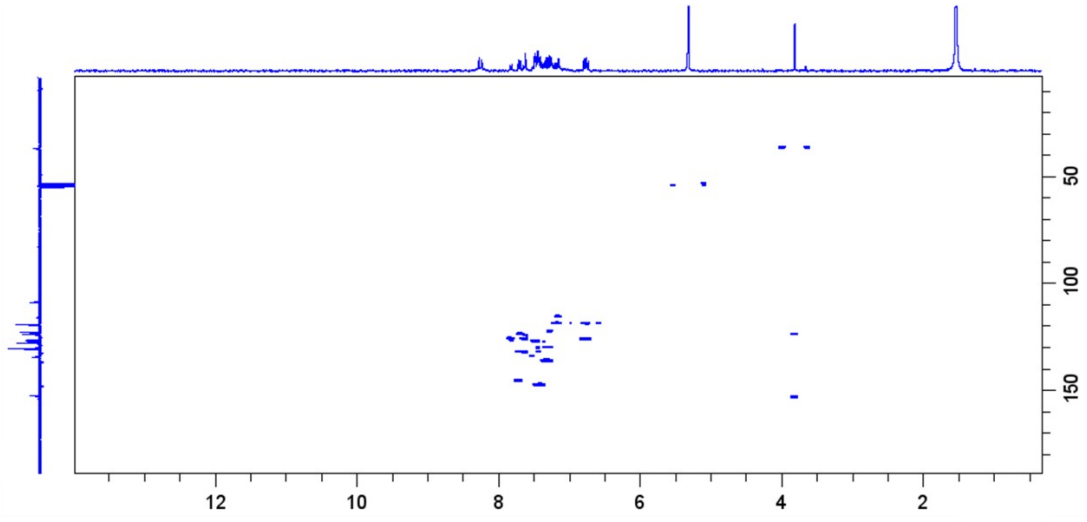

(d)

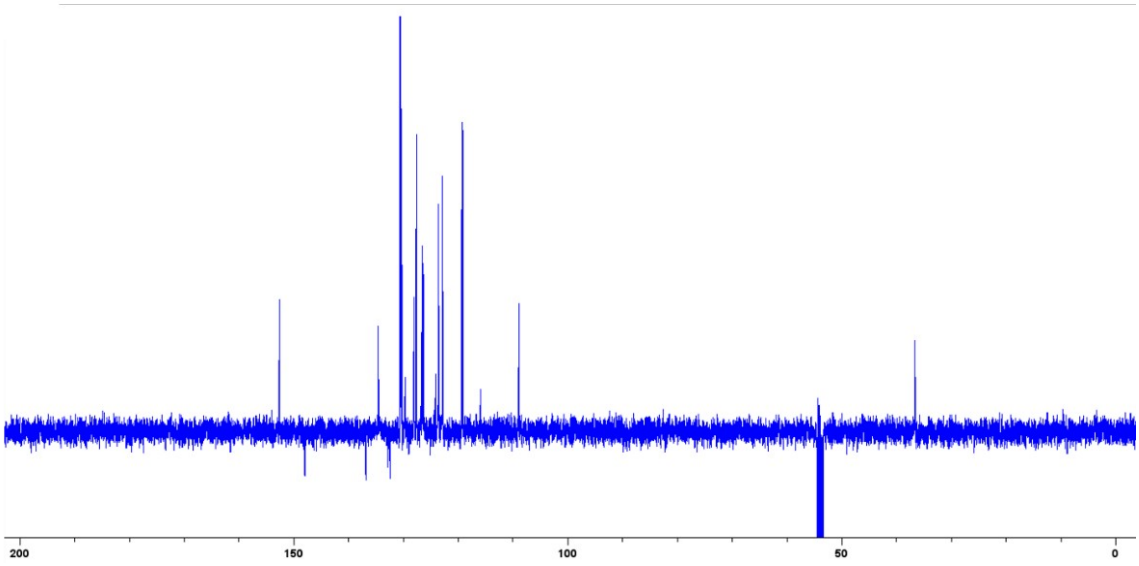

(e)

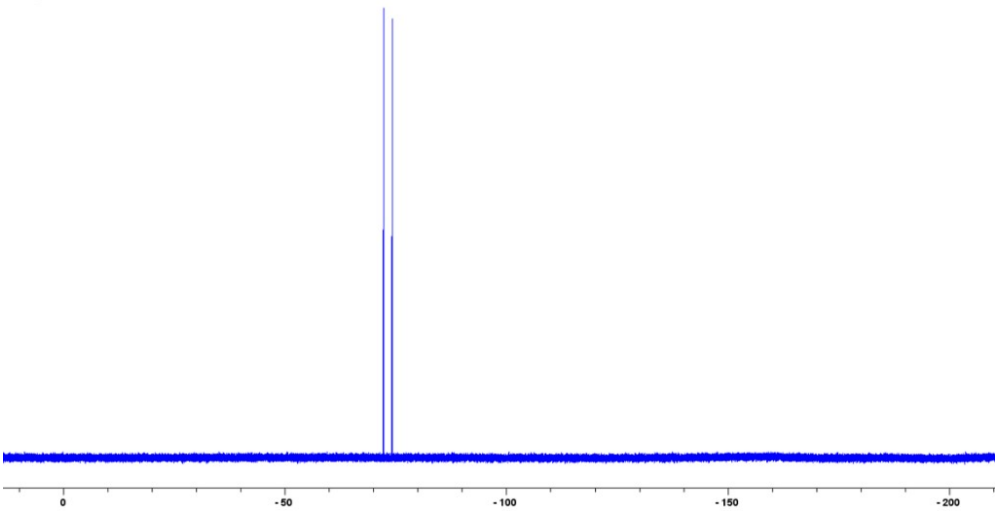

(f)

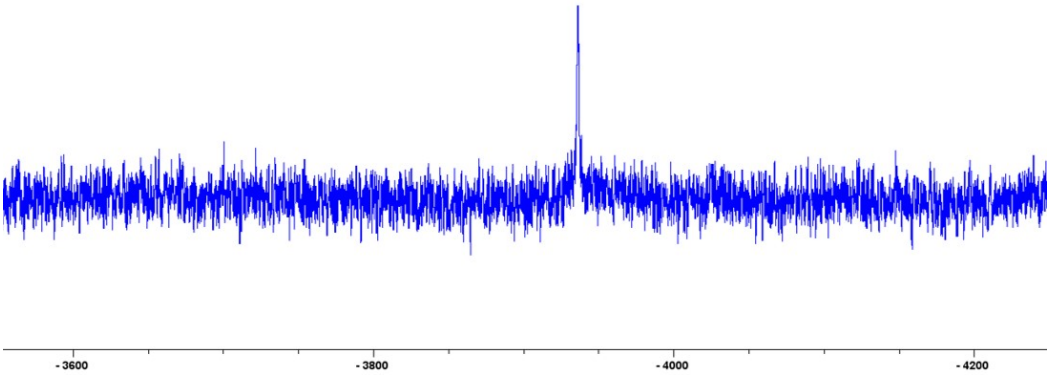

(g)

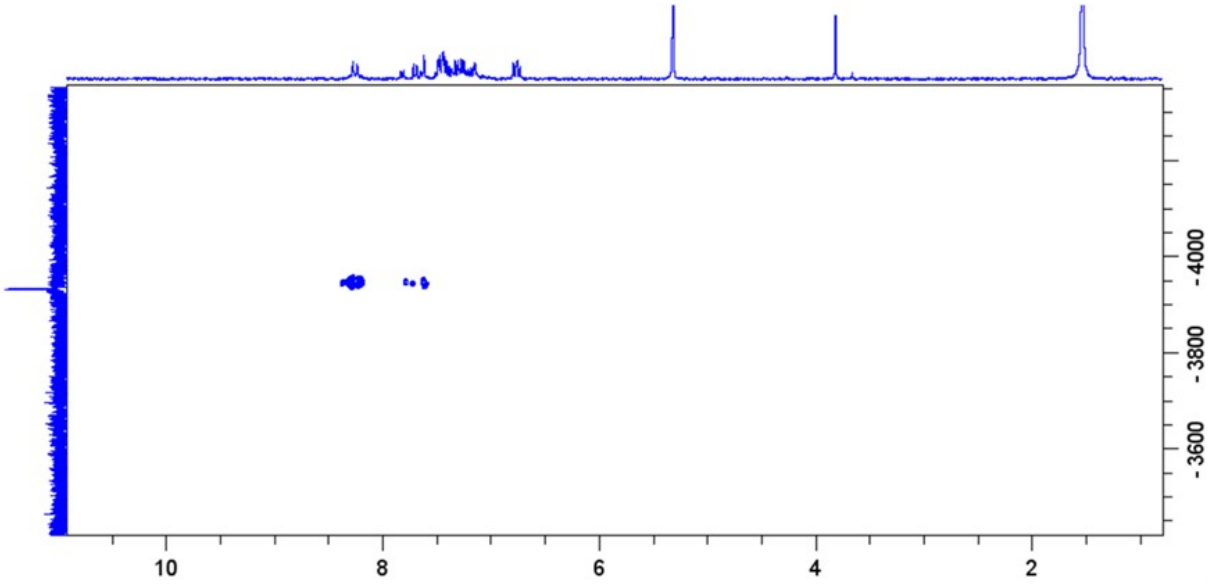

(h)

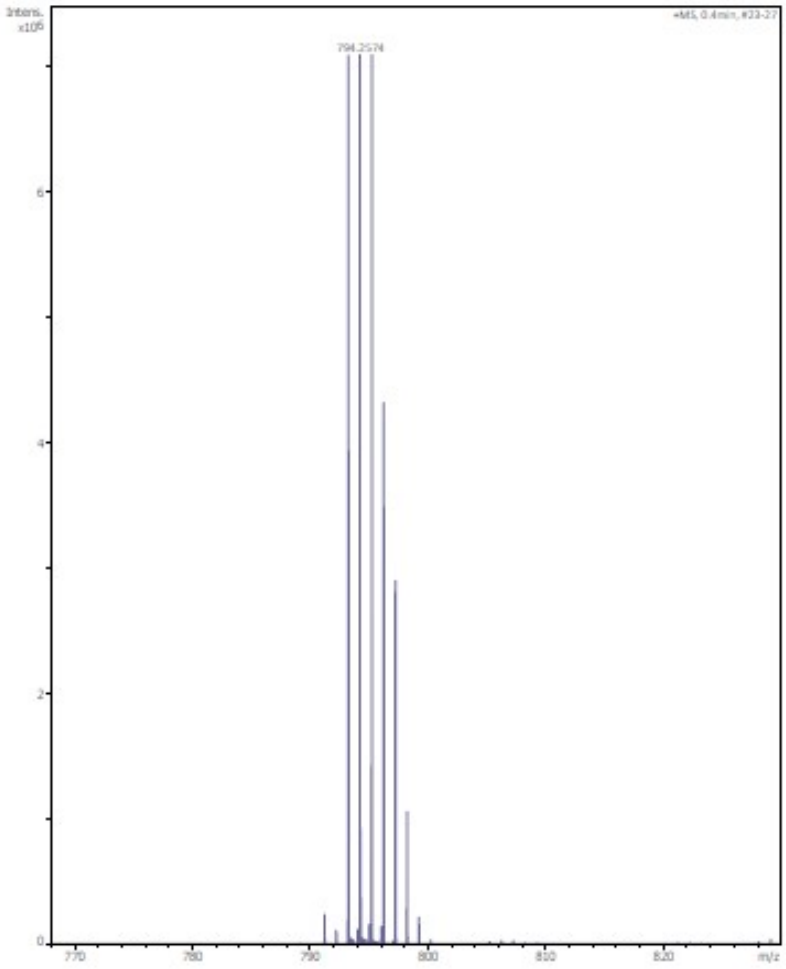

(i)

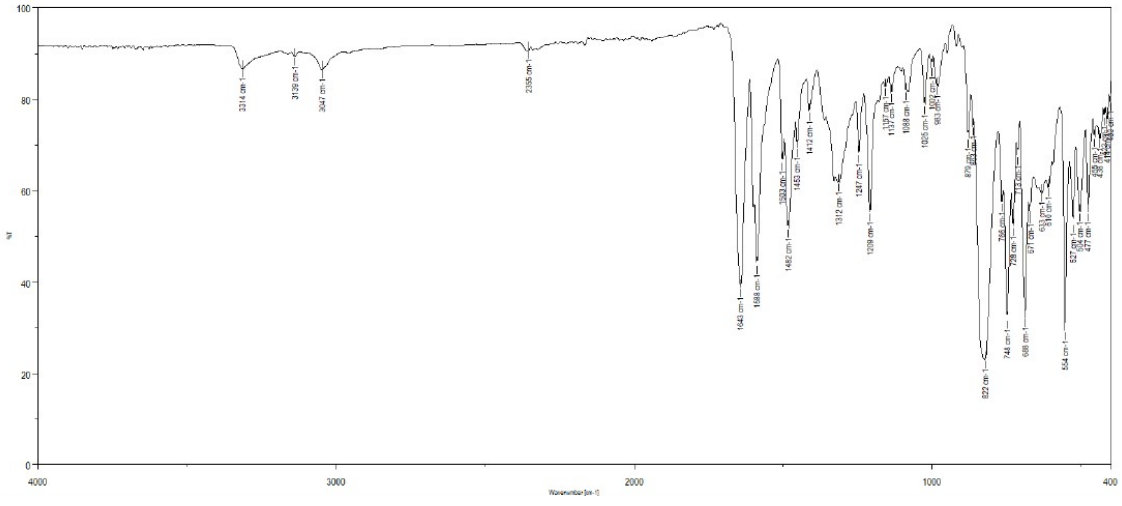

(j)

Figure S2. ^{1}H (a), ^{1}H-^{1}H COSY (b), ^{1}H -^{13}C HSQC (c), ^{1}H -^{13}C HMBC (d), $^{13}C\{^{1}H\}$ APT (e), $^{19}F\{^{1}H\}$ (f), $^{195}Pt\{^{1}H\}$ (g) ^{1}H -^{195}Pt HMQC (h) NMR spectra of **2** in CD_2Cl_2. MALDI+ MS (i) and IR (j) spectra of **2**.

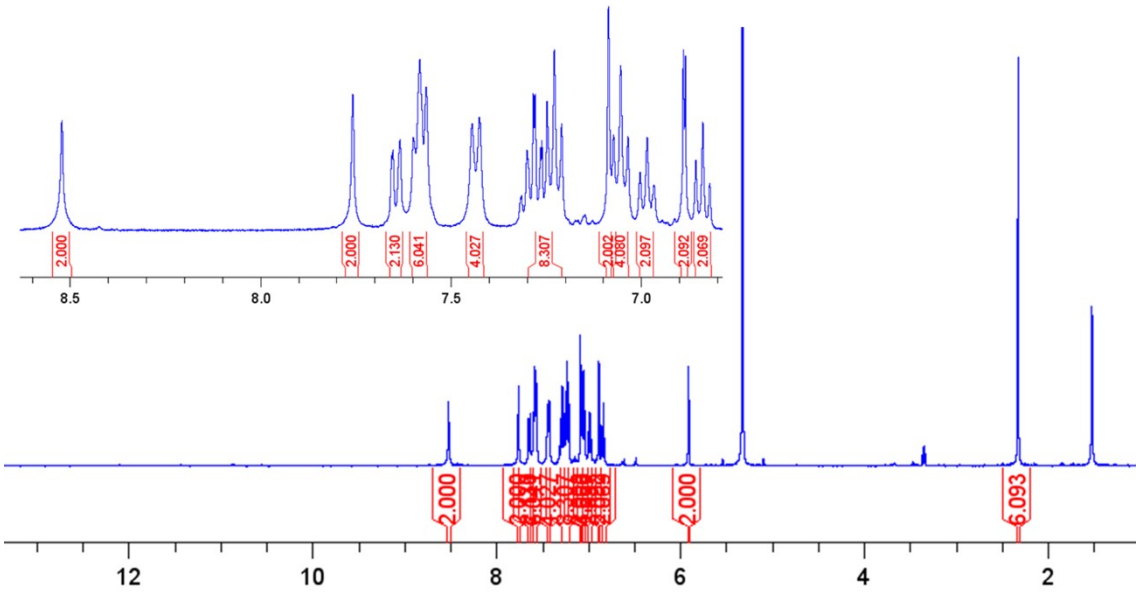
2.000
2.000
2.130
6.041
4.027
8.307
2.002
4.080
2.097
2.092
2.069
8.5
8.0
7.5
7.0
2.000
2.000
6.093
12
10
8
6
4
2

(a)

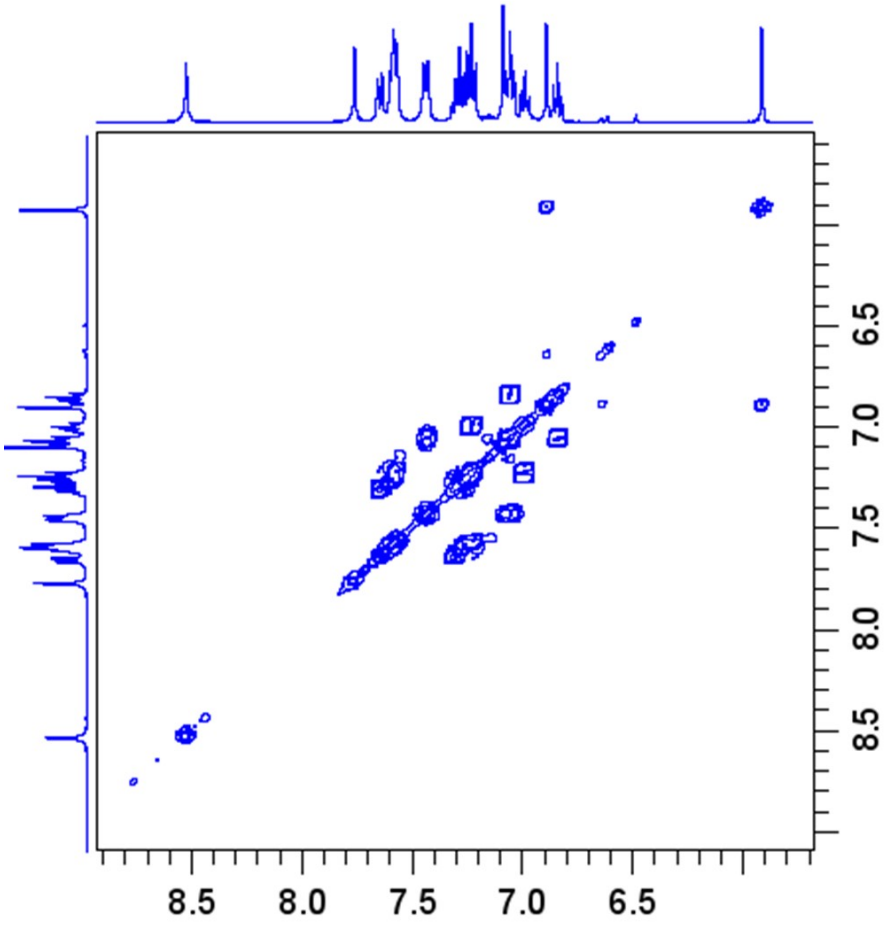
8.5
8.0
7.5
7.0
6.5

(b)

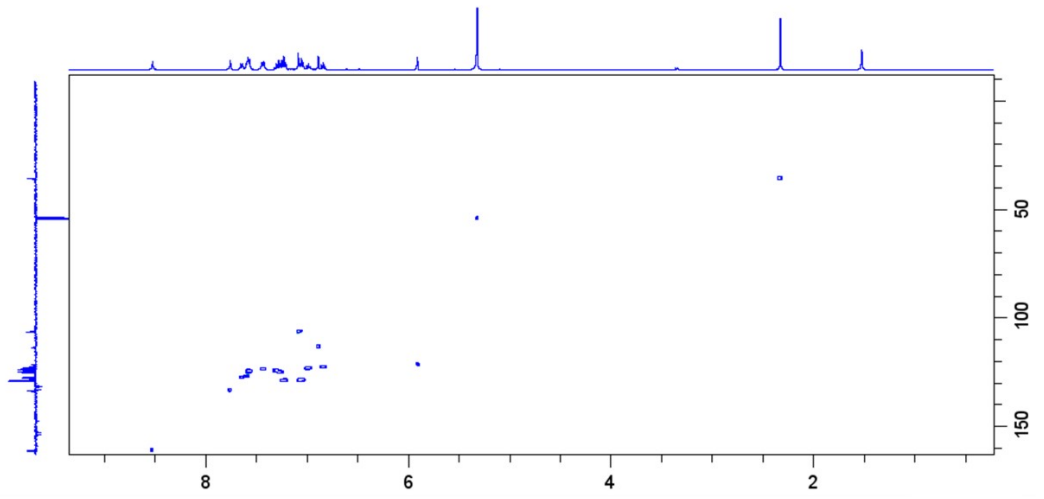

(c)

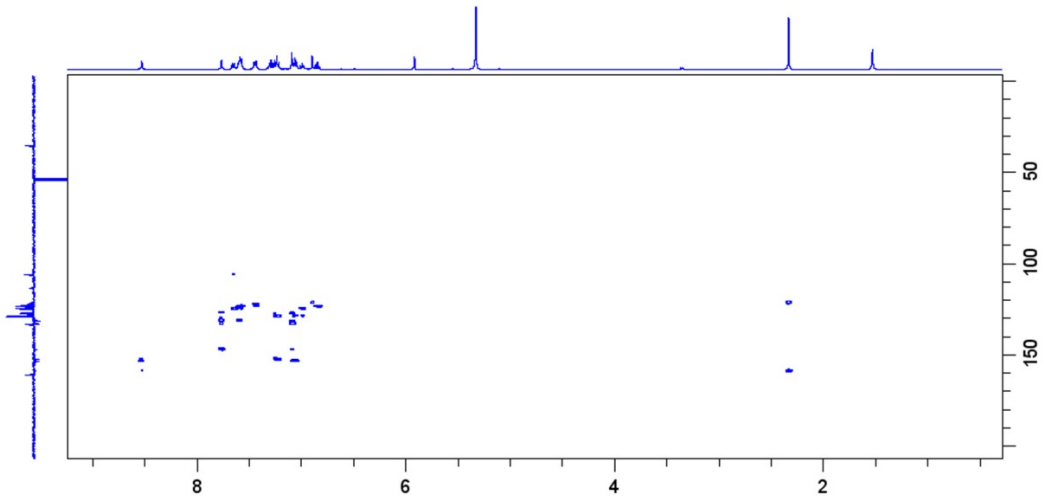

(d)

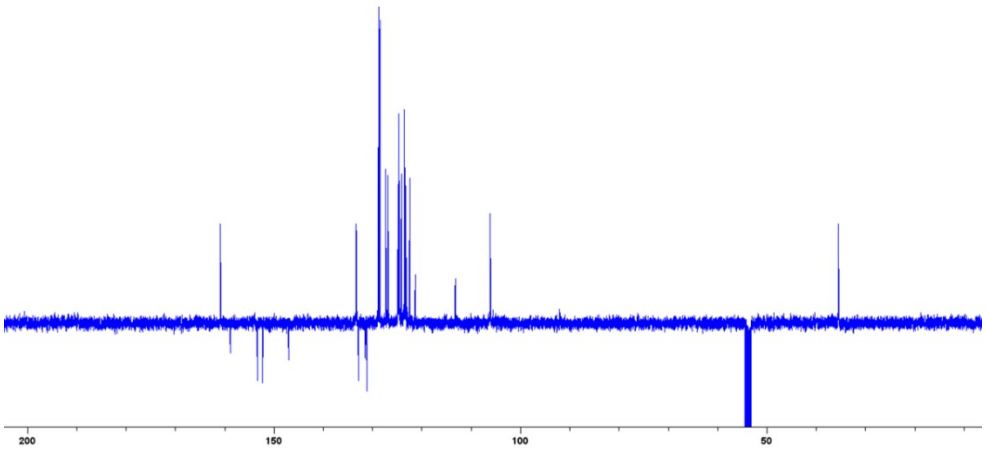

(e)

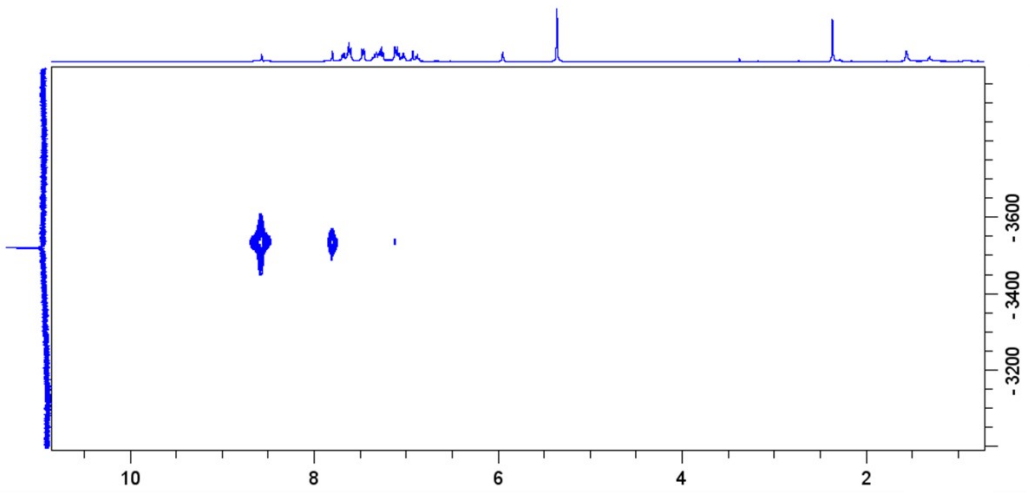

(f)

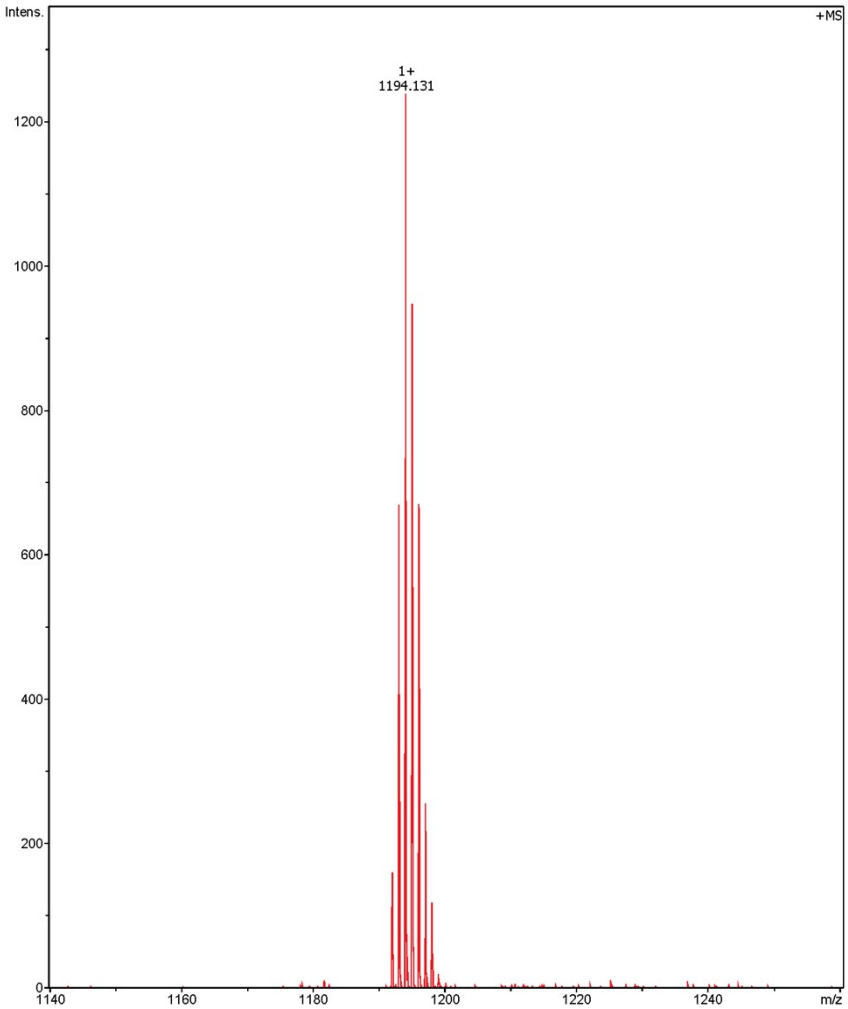

(g)

Figure S3. ^{1}H (a), ^{1}H-^{1}H COSY (b), ^{1}H -^{13}C HSQC (c), ^{1}H -^{13}C HMBC (d), $^{13}C\{^{1}H\}$ APT (e) ^{1}H -^{195}Pt HMQC (f) NMR spectra of **3** in CD_2Cl_2. MALDI+ MS spectra of **3** (g)

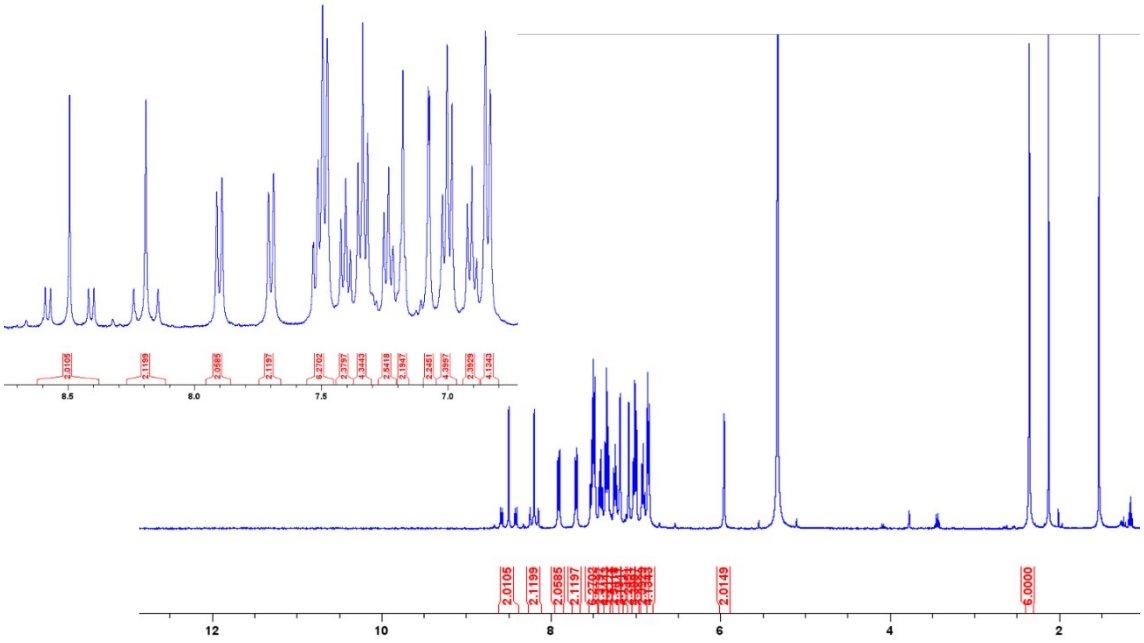
2.0105
2.1199
2.0585
2.1197
2.0149
6.0000
12
10
8
6
4
2

(a)

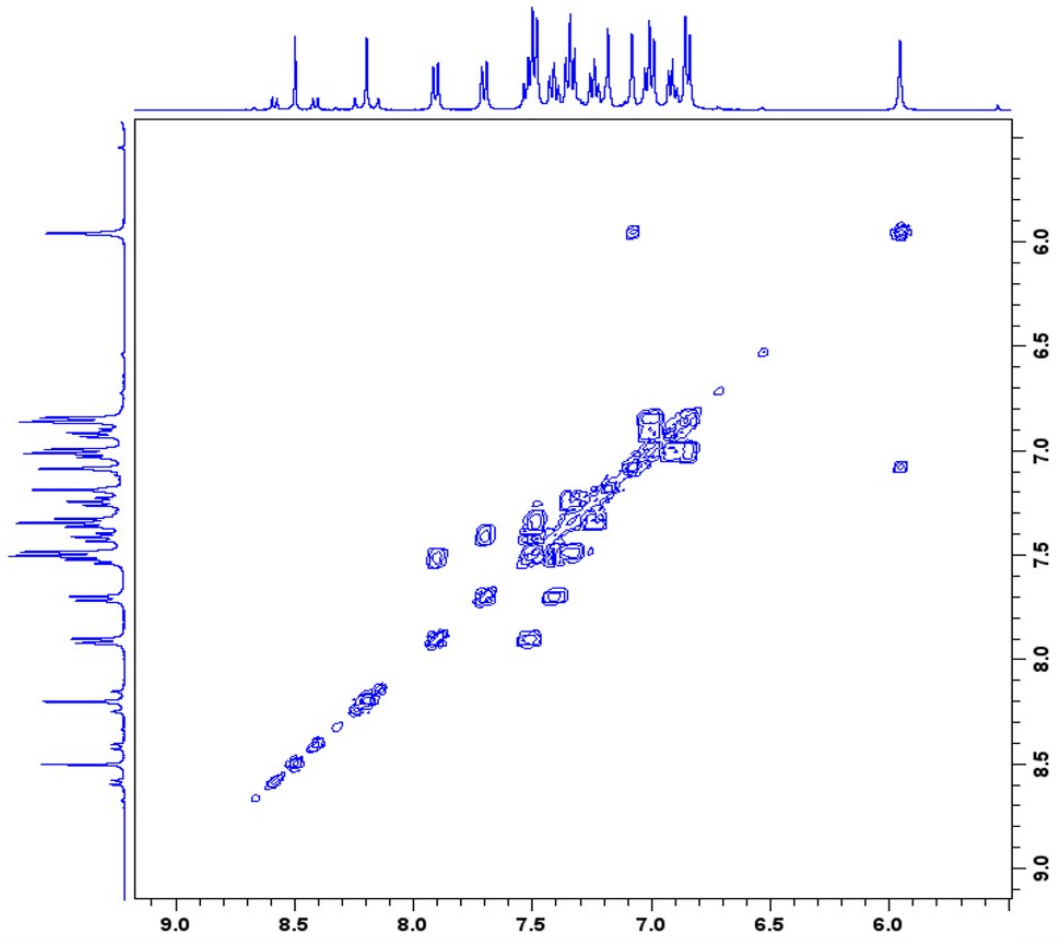
9.0
8.5
8.0
7.5
7.0
6.5
6.0

(b)

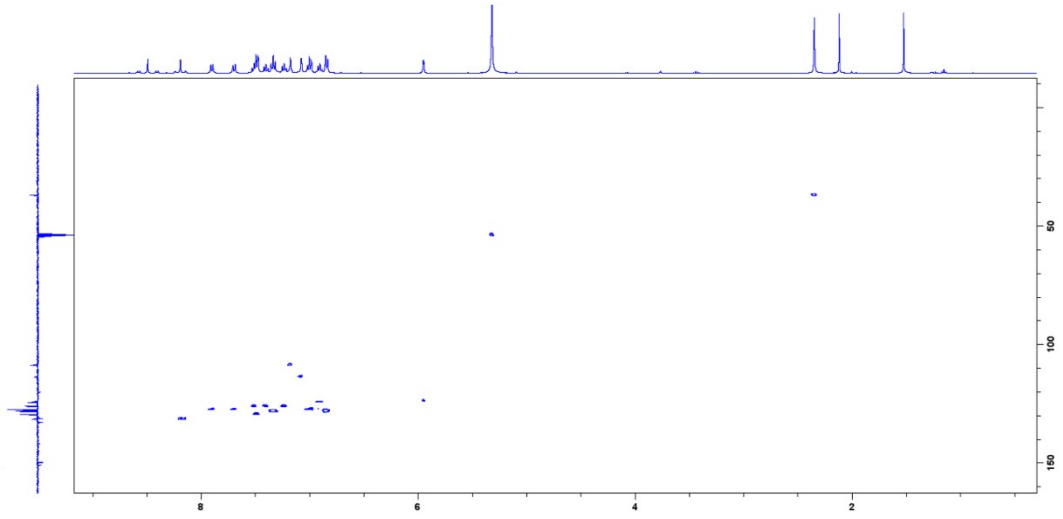

(c)

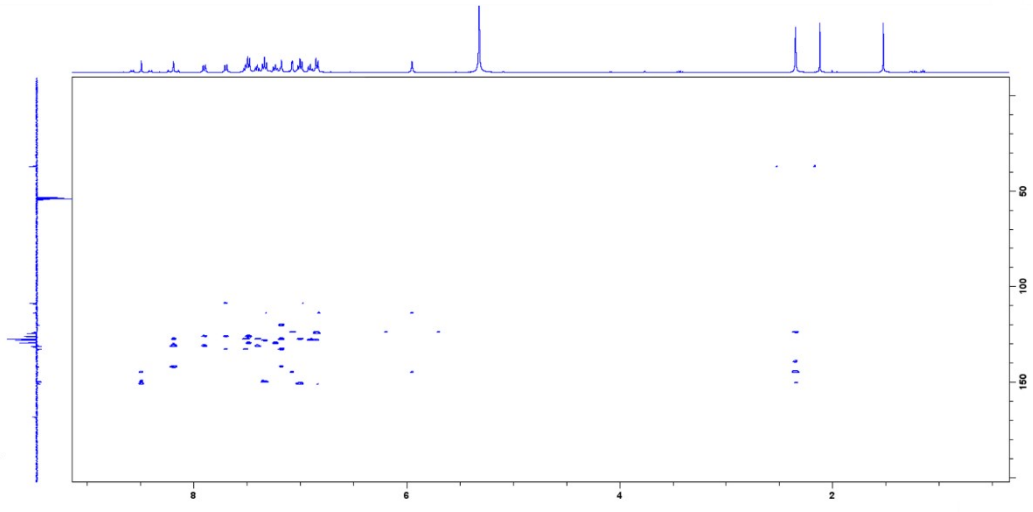

(d)

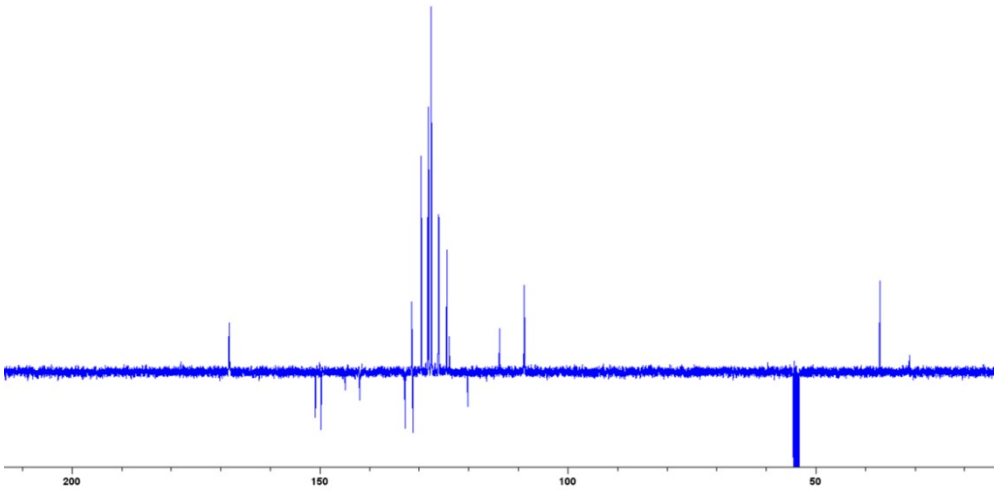

(e)

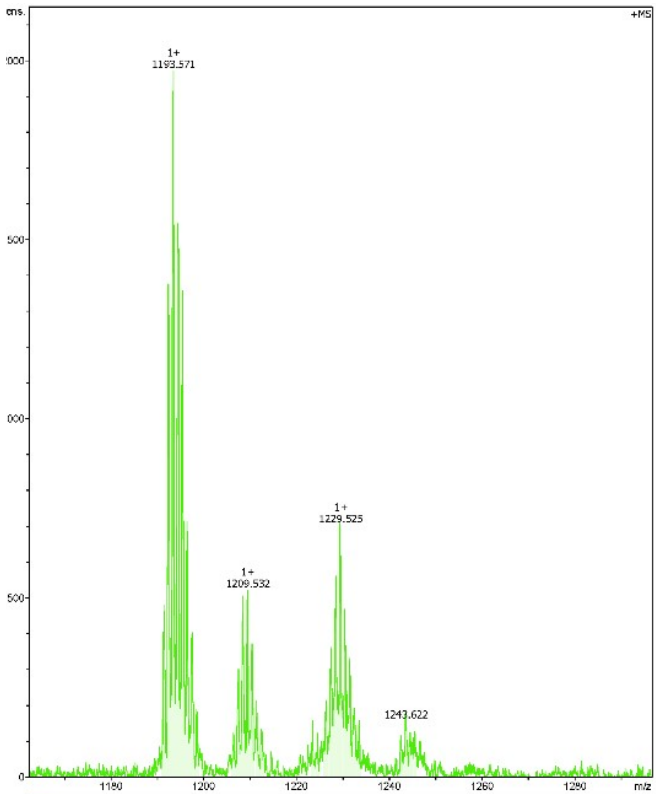

(f)

Figure S4. ^{1}H (a), ^{1}H-^{1}H COSY (b), ^{1}H -^{13}C HSQC (c), ^{1}H -^{13}C HMBC (d), ^{13}C{^{1}H} APT (e) NMR spectra of **4-Cl** in CD_2Cl_2. MALDI+ MS spectra of **4-Cl** (f)

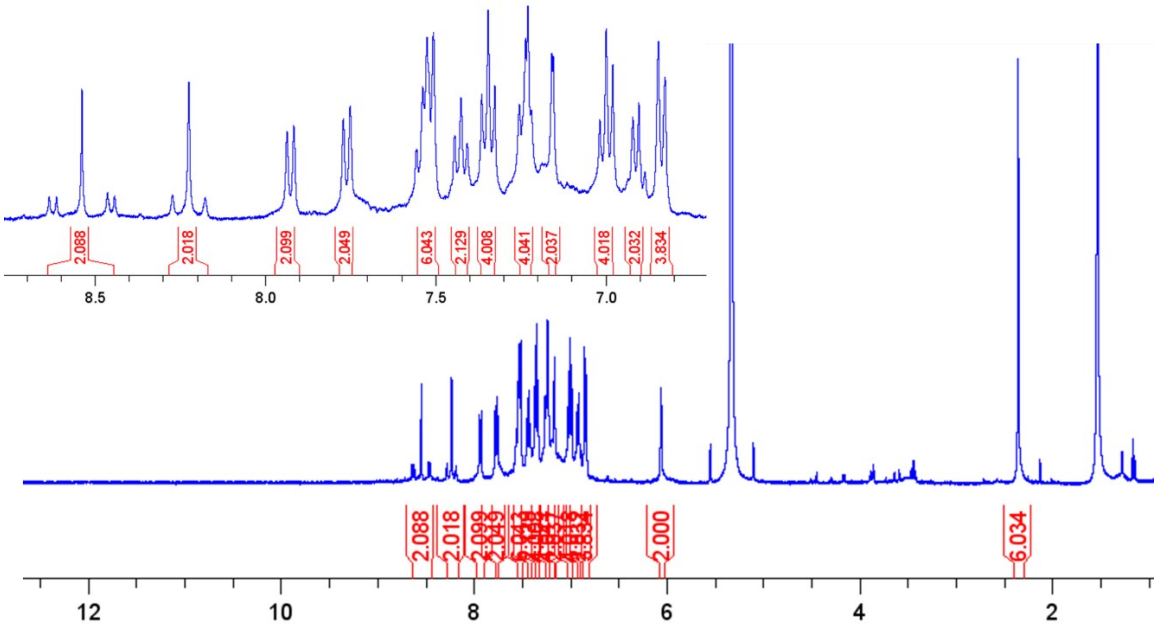
2.088
2.018
2.099
2.049
6.043
2.129
4.008
4.041
2.037
4.018
2.032
3.834
8.5
8.0
7.5
7.0
2.088
2.018
2.000
6.034
12
10
8
6
4
2

(a)

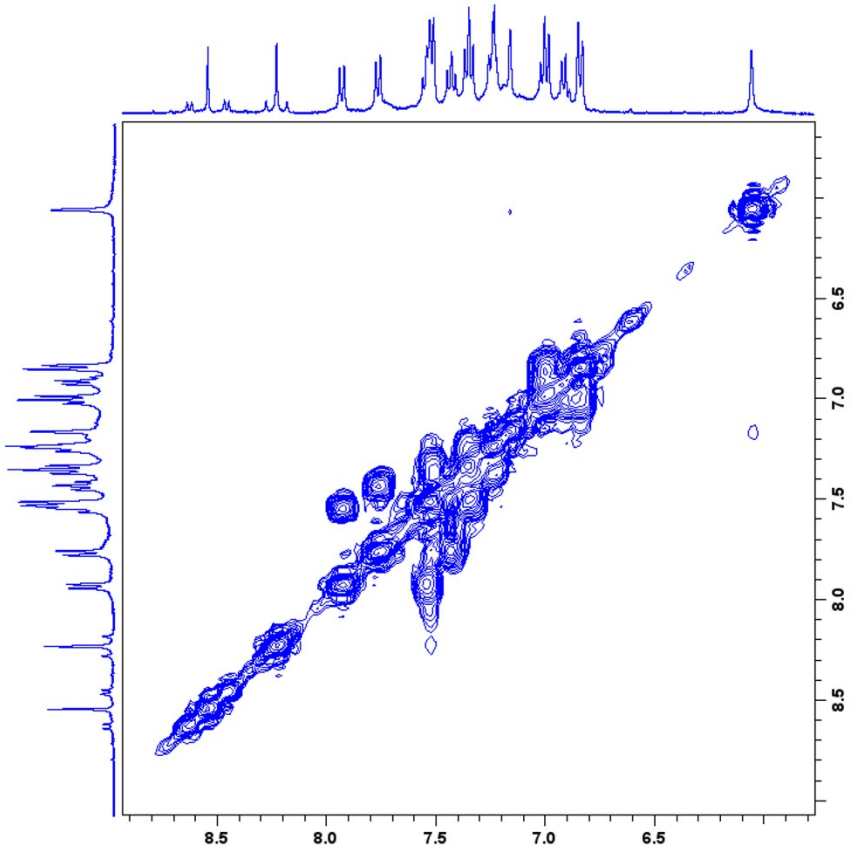
8.5
8.0
7.5
7.0
6.5
6.5
7.0
7.5
8.0
8.5

(b)

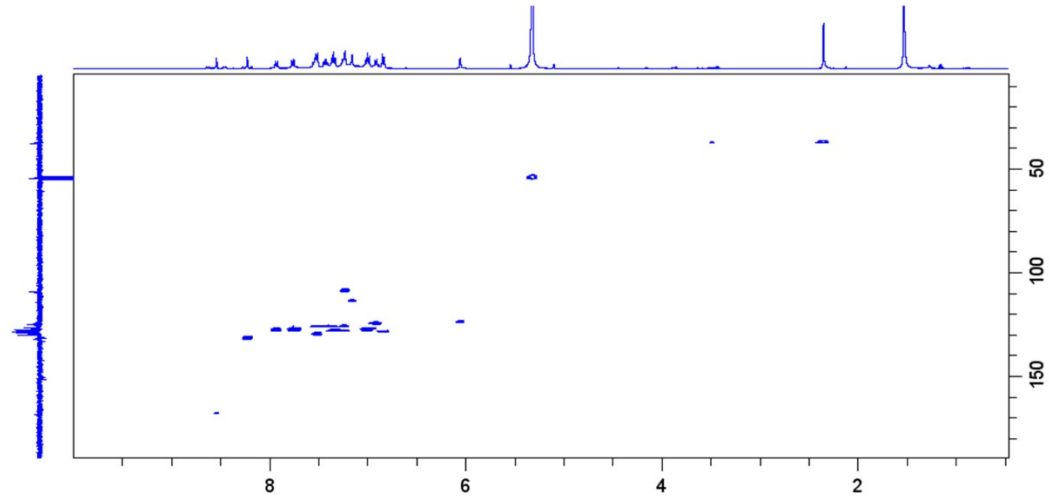

(c)

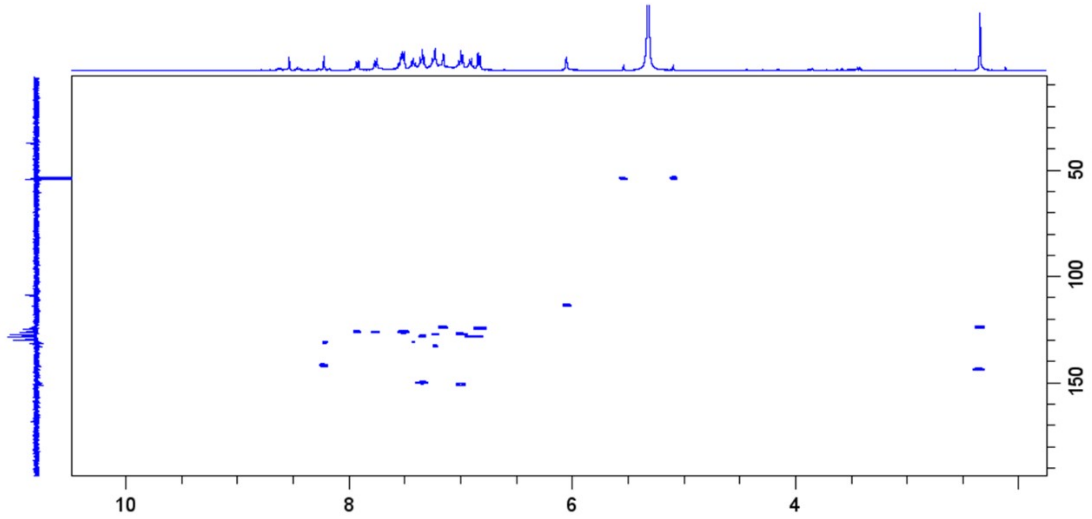

(d)

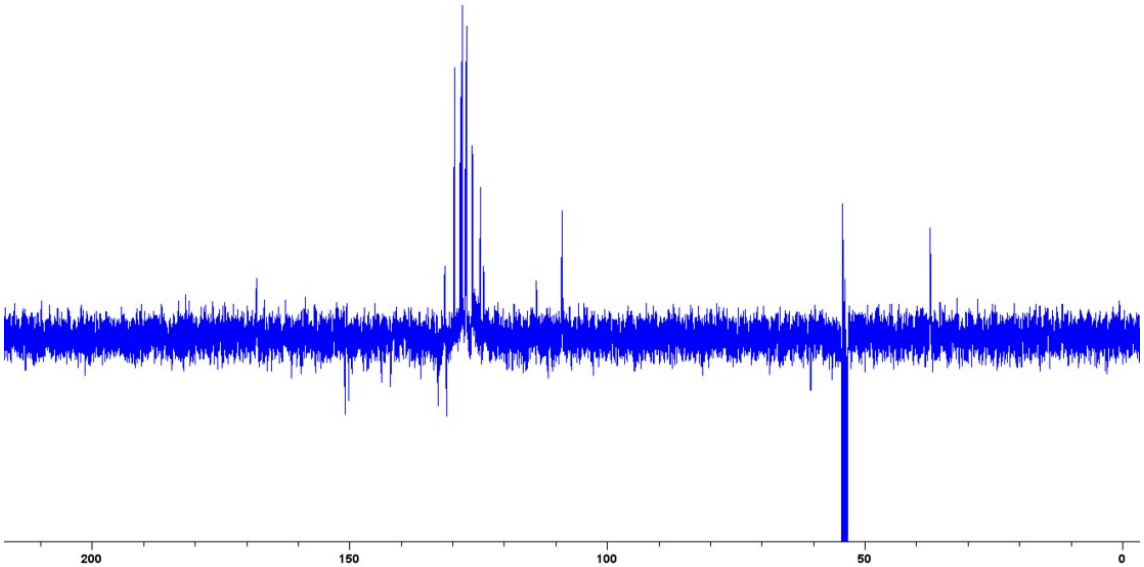

(e)

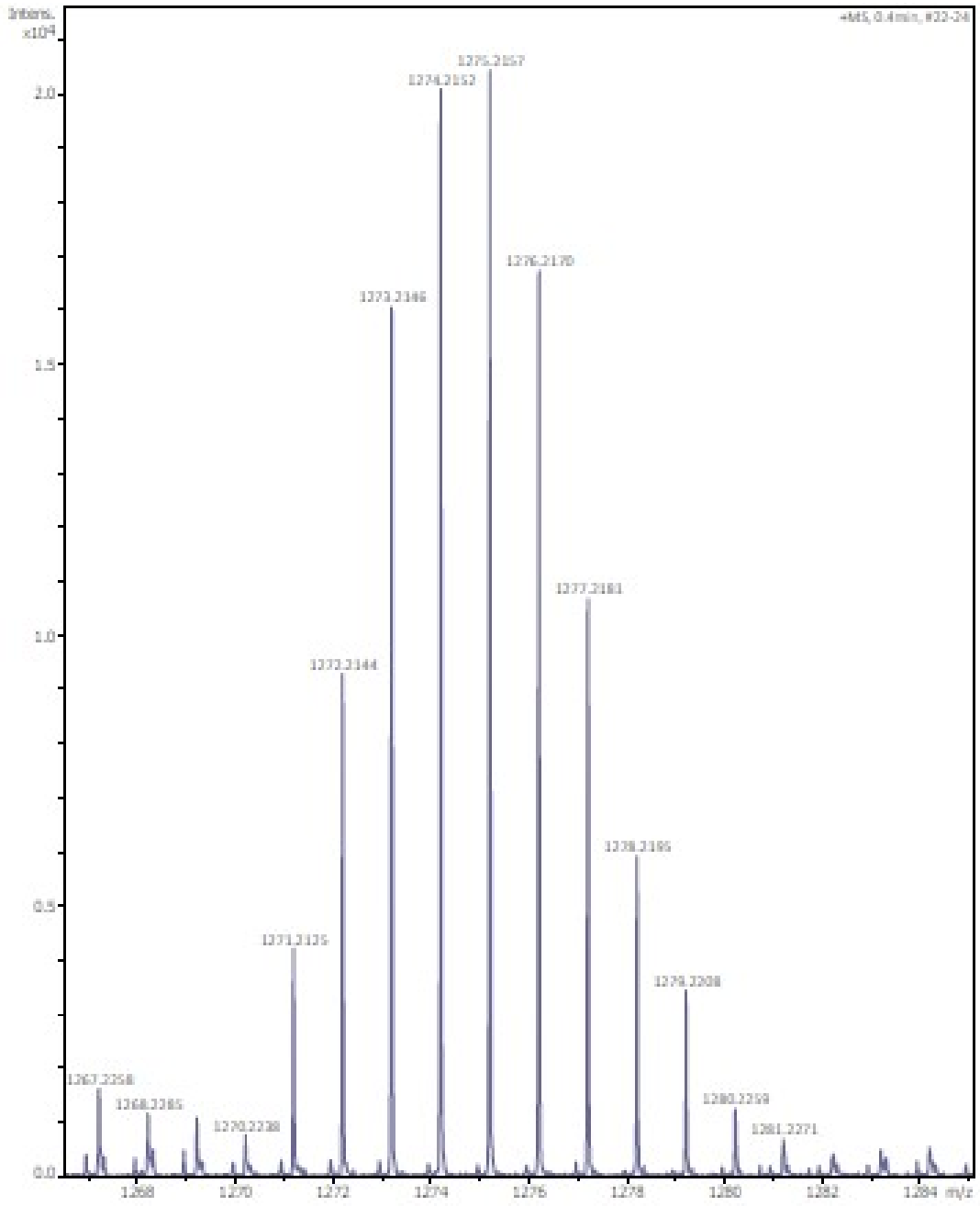

(f)

Figure S5. ^{1}H (a), ^{1}H-^{1}H COSY (b), ^{1}H -^{13}C HSQC (c), ^{1}H -^{13}C HMBC (d), $^{13}C\{^{1}H\}$ APT (e) NMR spectra of **4-Br** in CD_2Cl_2. MALDI+ MS spectra of **4-Br** (f)

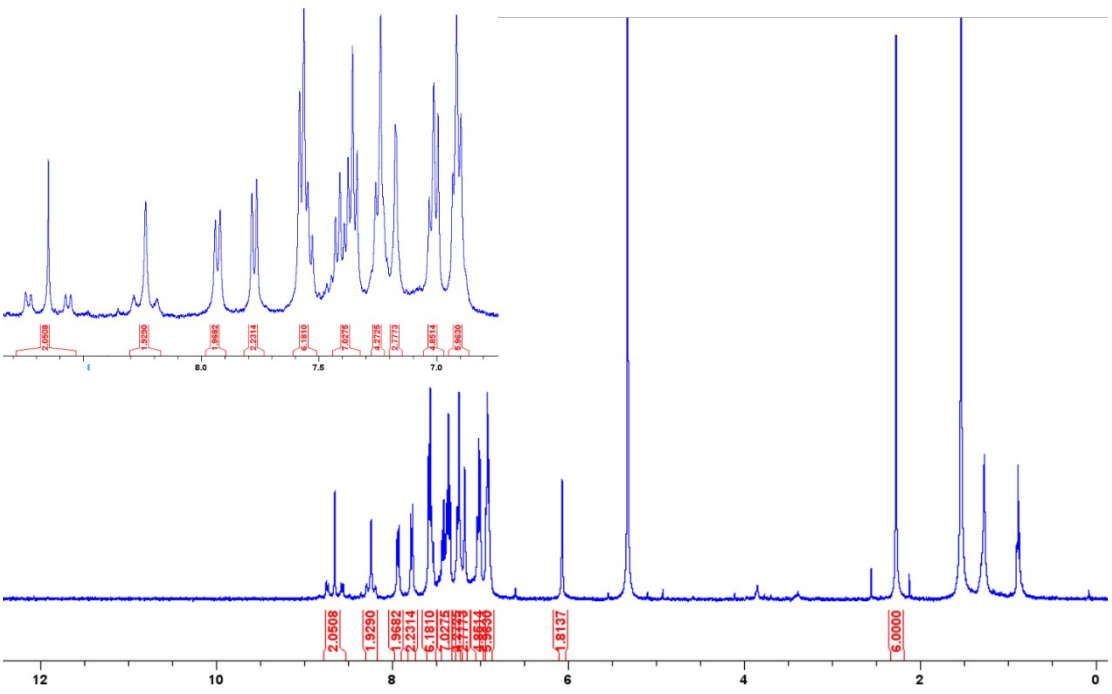

(a)

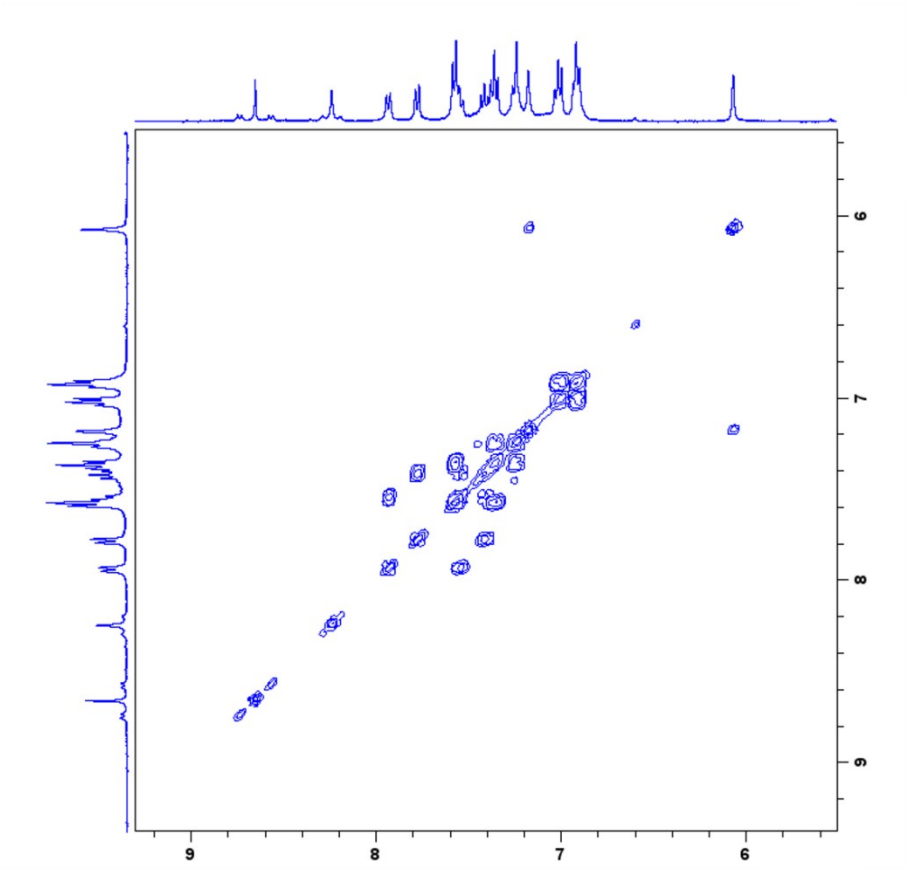

(b)

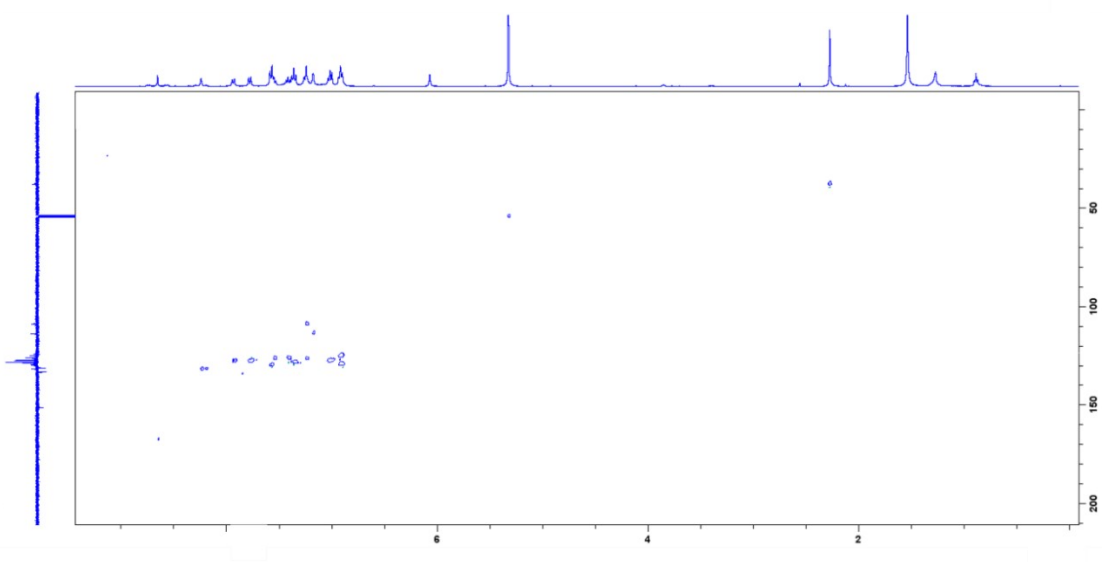

(c)

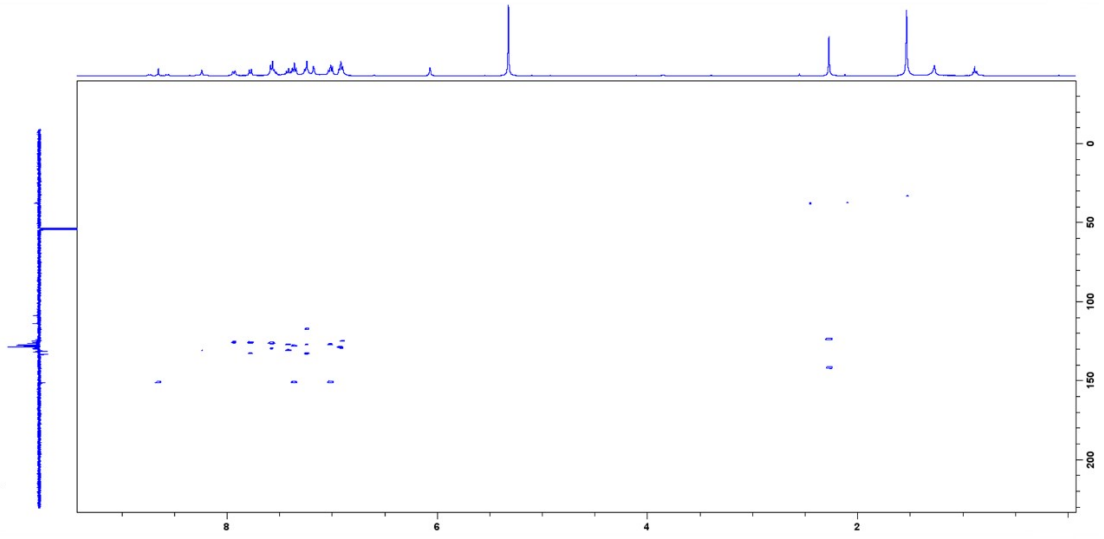

(d)

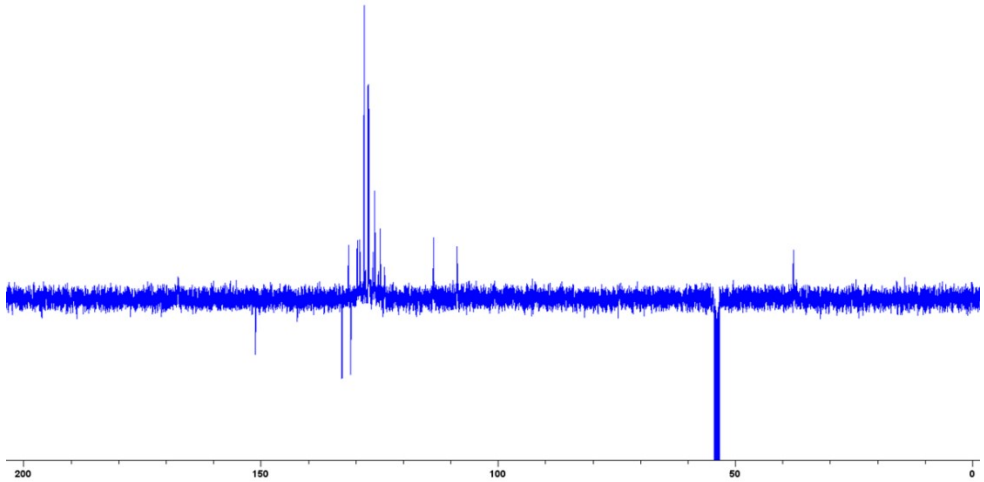

(e)

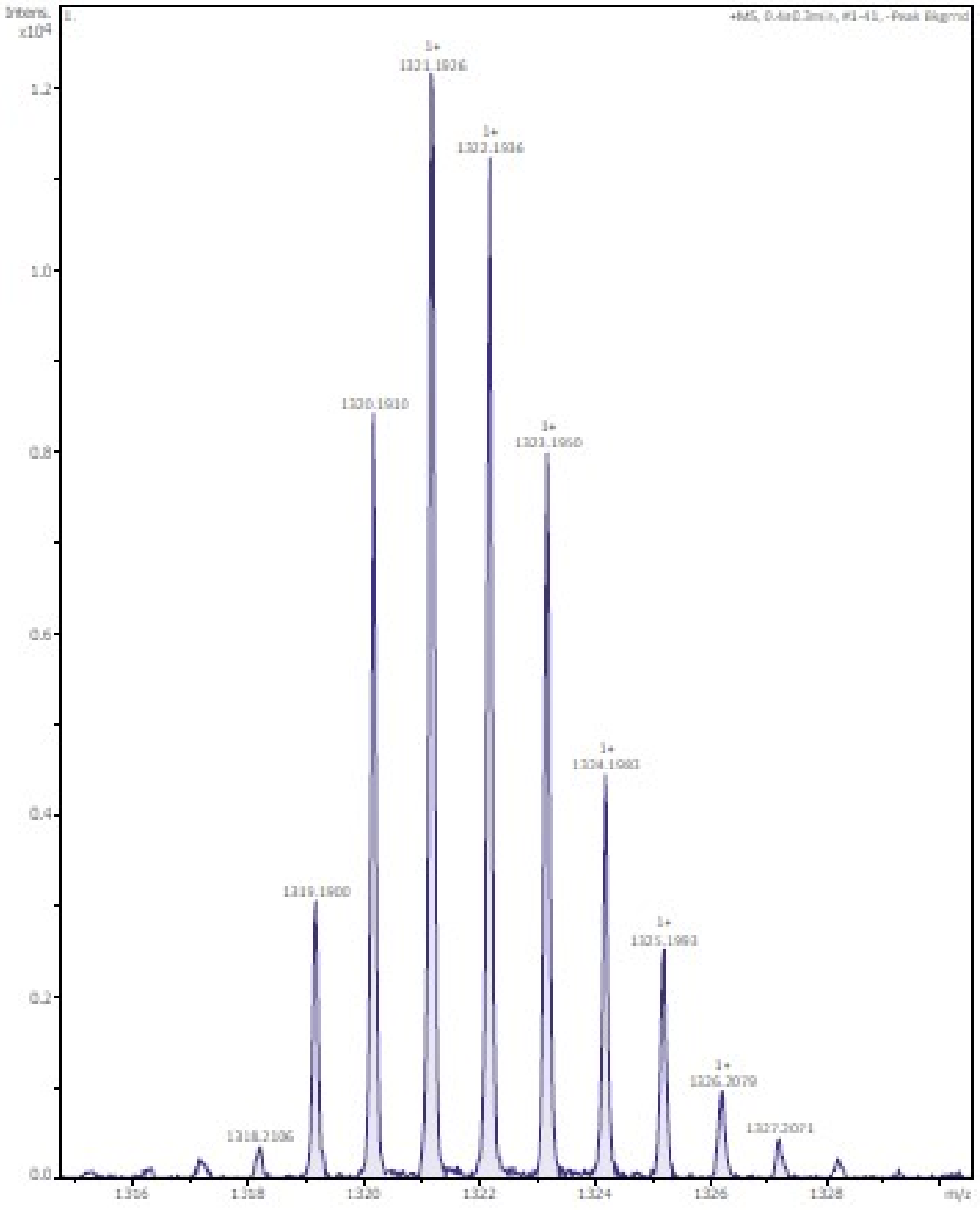

(f)

Figure S6. ^{1}H (a), ^{1}H-^{1}H COSY (b), ^{1}H -^{13}C HSQC (c), ^{1}H -^{13}C HMBC (d), $^{13}C\{^{1}H\}$ APT (e) NMR spectra of **4-I** in CD_2Cl_2. MALDI+ MS spectra of **4-I** (f)

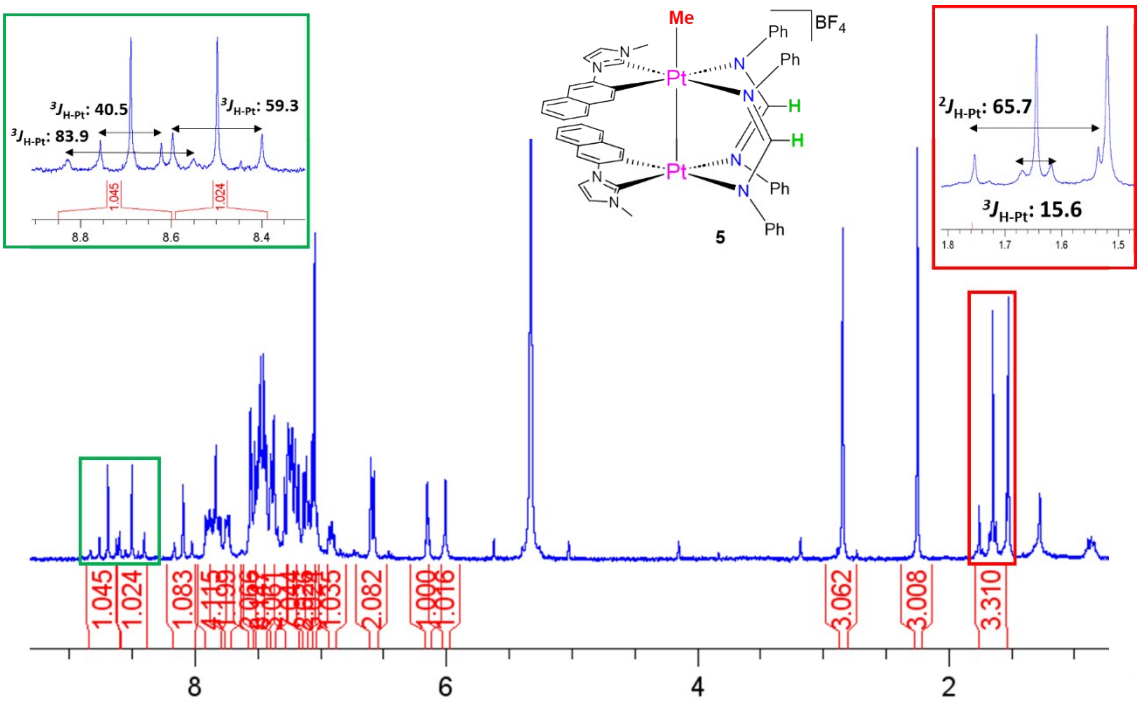
Me
BF4
Ph
Ph
Pt
N
H
5
3J H-Pt: 40.5
3J H-Pt: 59.3
3J H-Pt: 83.9
2J H-Pt: 65.7
3J H-Pt: 15.6
1.045
1.024
1.083
2.082
1.000
1.016
3.062
3.008
3.310
8
6
4
2

(a)

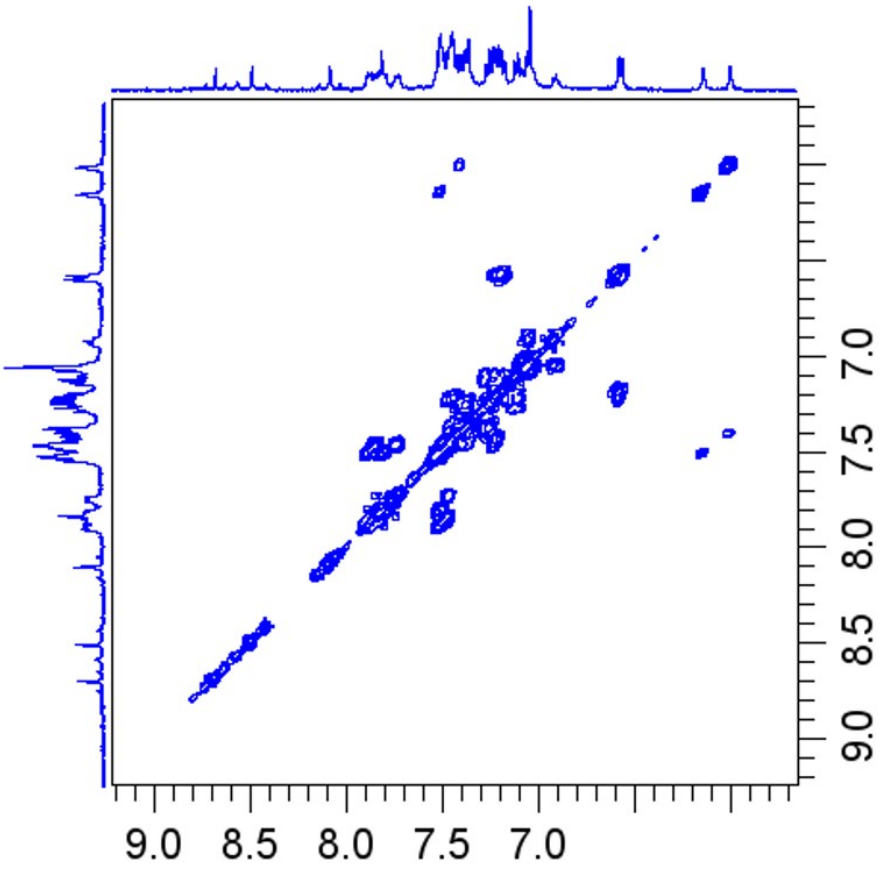
9.0
8.5
8.0
7.5
7.0

(b)

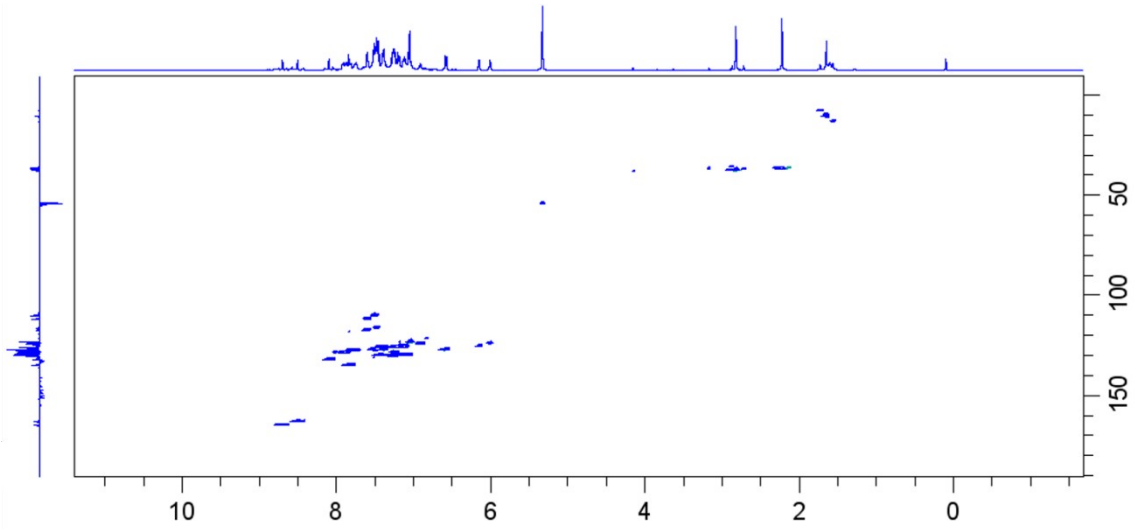

(c)

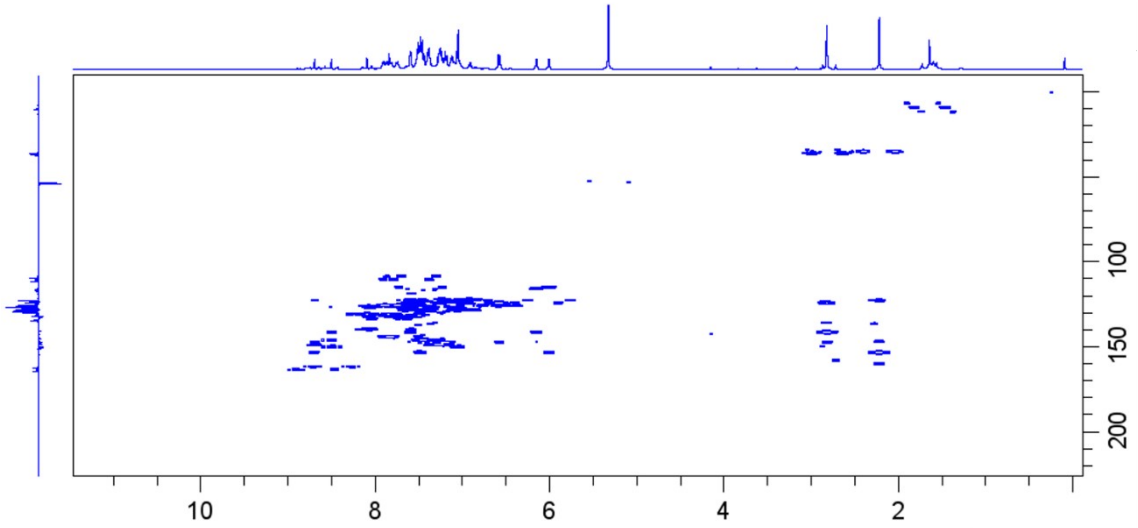

(d)

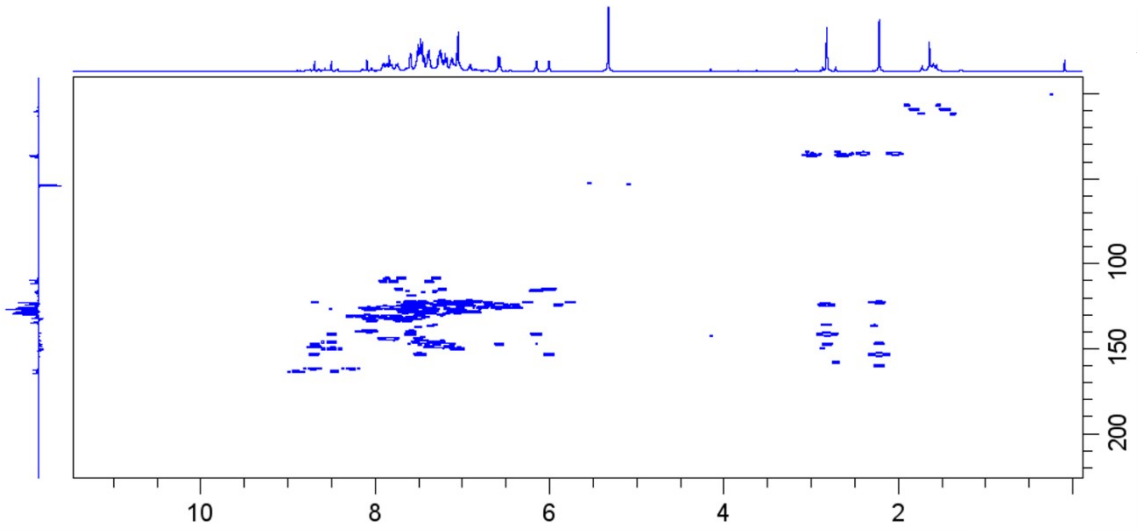

(e)

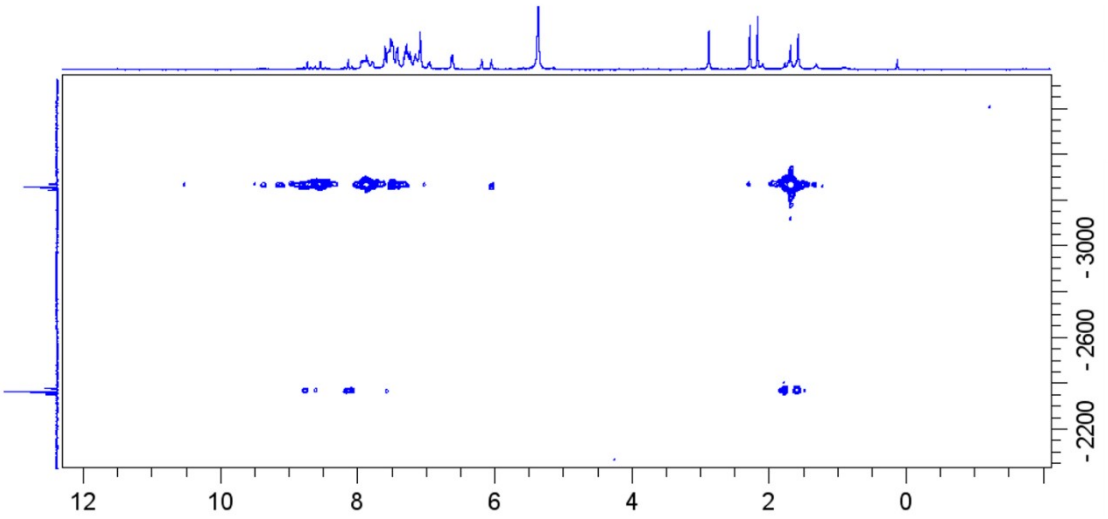

(f)

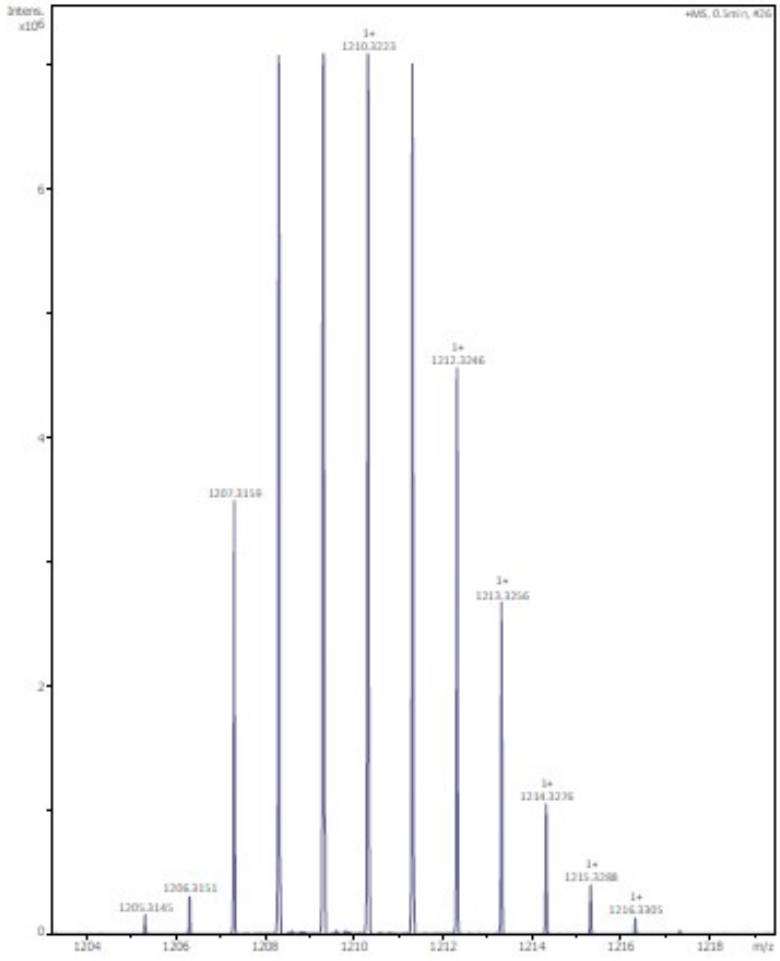

(g)

Figure S7. ^{1}H (a), ^{1}H-^{1}H COSY (b), ^{1}H -^{13}C HSQC (c), ^{1}H -^{13}C HMBC (d), $^{13}C\{^{1}H\}$ APT (e), HMQC ^{1}H -^{195}Pt (f) NMR spectra of **5** in CD_2Cl_2. MALDI+ MS spectra of **5** (g)

3. X-RAY DIFFRACTION STUDIES FOR CHARACTERIZATION

The X-ray molecular structures of complexes **3**, **4-Cl** and **4-I** have been depicted in Figures 5 and S8 and a selection of bond distances and angles appears listed in Table S2. Although high-quality crystals of **4-I** could not be obtained, the atom connectivity was successfully determined. The asymmetric unit of **4-Cl** contains two dinuclear molecules (A and B) with very similar bonding parameters; thus only one set of data, (PtA) is included here. As shown in Figure 5, complex **3** is formed by two Pt(C^C*) units doubly bridged with two 2-fomamidinates. Both Pt(II) centers coordinate to the two carbon atoms of the cyclometallated moiety and two N atoms, one of each formamidinate. The square-planar coordination of the metal shows a considerable distortion because of the constrained angle of the C^C* chelating ligand [*ca.* 80º]. These C^C* fragments display an *anti*-arrangement and the platinum coordination planes are not completely parallel to one another, with a dihedral angle of 19.5º. The metal centers are in close proximity with a Pt-Pt distance of 2.86457(17) Å, like in similar amidinate dinuclear complexes,[11-17] denoting a strong interaction of the $5dz^2$ orbitals of both platinum centers.

X-ray diffraction studies on **4-Cl** and **4-I** confirmed that the oxidation of **3** proceeds with retention of the conformation, obtaining the *anti*-isomer for both complexes. The Pt(III) centers have a distorted octahedral environment with the axial positions occupied by a halogen atom and the other Pt(III) center and with the X−Pt−Pt angles being close to 177° (X: Cl). The Pt-Pt distance 2.6070(5) Å is smaller than that of complex **3**, in accordance with the presence of a metal-metal bond between both Pt(III) centers and lays within the range observed for analogous complexes $[\{Pt^{III}(C^N)(\mu\text{-}S^N)Cl\}_2]$ with C^N-cyclometallated groups and four-bond bridging ligands (S^N).[18-23] The two Pt coordination planes are approximately parallel as evidenced by the small dihedral angle

[13.2(2)º], with the Cl-Pt-Pt-Cl vector oriented almost orthogonally to both planes [6.7(2)º and 6.4(2)º].

The bonding parameters of the five membered metallocycle in complexes **2**, **3** and **4-Cl** are analogous to those found for related (C^C*)Pt(II)[1, 24, 25] and (C^C*)Pt(III)[25-27] complexes. Regarding the Pt-N distances, the Pt-$N_{trans\text{-}CAr}$ is somewhat longer than that for Pt-$N_{trans\text{-}C*}$, in agreement with the higher *trans* influence of the C_{Ar} when compared to the carbenic one (C*).[28] A deeper examination of the crystal structures revealed in **3** and **4-Cl** π-π intermolecular interactions (3.27-3.51 Å, cyan dotted lines, insets Figure 5) between the C^C* fragments of adjacent molecules, leading to the formation of 1D-stackings. In **4-Cl**, this supramolecular array is also supported by H···Cl interactions (d H-Cl: 2.628 Å, d C-Cl: 3.464 Å) between the C^C* and the axial Cl ligands.

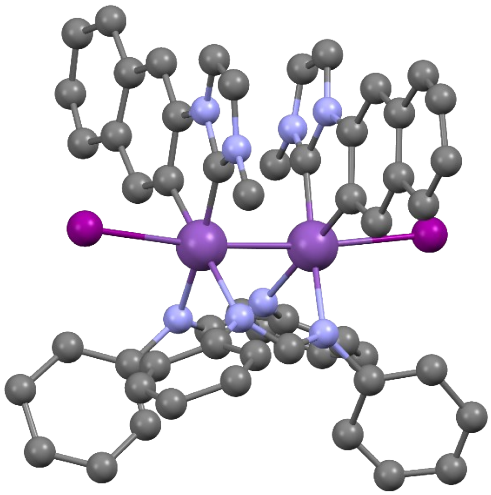

Figure S8. X-ray molecular structure of **4-I.** Thermal ellipsoids are drawn at their 50% probability level, solvent molecules and hydrogens are omitted for clarity.

Table S2. Selected bond lengths (Å) and angles (°) of complex **2**, **3** and **4-Cl**

Distances (Å)	**2**	**3**	**4-Cl (Pt1A/Pt2A)**
Pt-Pt		2.86457(17)	2.6070(5)
Pt-C1(C^*)	1.983(6)	1.965(2)	1.989(6) / 1.987(6)
Pt-C6(C_{ar})	2.014(6)	1.998(2)	2.024(6) / 2.032(7)
Pt-$N_{trans\text{-}Car}$	2.129(5)	2.1311(17)	2.173(6) / 2.178(6)
Pt-$N_{trans\text{-}C*}$	2.092(6)	2.0946(18)	2.072(5) / 2.077(5)
Pt-Cl			2.4510(18) / 2.4379(17)
Angles (°)			
C^*-Pt-C_{ar}	80.3(2)	80.13(9)	80.6(3) / 79.3(3)
$N_{t\text{-}Car}$-Pt-C^*	100.9(2)	101.69(8)	102.2(2) / 103.4(2)
$N_{t\text{-}C*}$-Pt-$N_{t\text{-}Car}$	83.1(2)	84.28(7)	84.9(2) / 83.4(2)
C_{ar}-Pt-$N_{t\text{-}C*}$	95.7(2)	94.12(8)	92.4(2) / 93.8(2)
C_{ar}-Pt-Cl			85.081(18) / 87.76(18)
C^*-Pt-Cl			83.10(18) / 82.95(18)
$N_{t\text{-}C*}$-Pt-Cl			94.34(17) / 96.94(16)
$N_{t\text{-}Car}$-Pt-Cl			98.53(16) / 97.30(16)
Pt-Pt-Cl			176.44(5) / 177.90(4)

3. Photophysical, electrochemical and theoretical studies

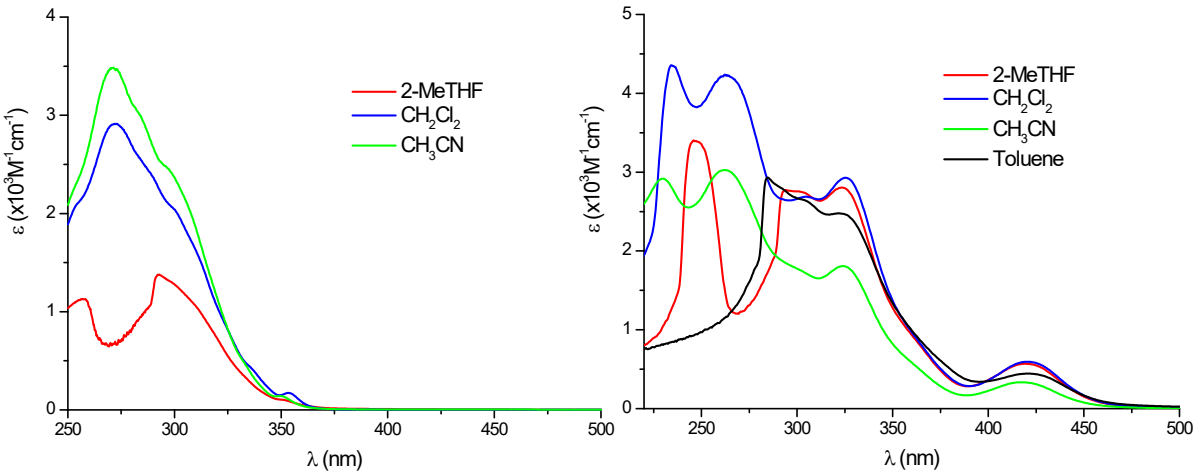

Figure S9. UV-Vis spectra of **2** (left) and **3** (right) in different solvents at $5x10^{-5}$ M.

Table S3. Absorption data in solution ($5 \cdot 10^{-5}$ M) at 298 K.

Compound	**λ /nm (10^3 ε M^{-1} cm^{-1})**
2	257 (22.6), 284 (18.9), 293 (27.5), 311_{sh} (20.6), 351 (2.1) **2-MeTHF** 272 (58.3), 288_{sh} (48.6), 300_{sh} (40.8), 337_{sh} (8.1), 354 (3.4) **CH_2Cl_2** 271 (69.6), 283_{sh} (60.6), 297 (49.1), 350 (2.8) **CH_3CN**
3	247 (67.9), 294 (55.5), 302_{sh} (55.0), 324 (56.1), 420 (11.4) **2-MeTHF** 234 (87.0), 262 (84.7), 305 (53.8), 325 (58.6), 420 (11.9) **CH_2Cl_2** 230 (58.3), 262 (60.5), 297 (36.2), 324 (36.2), 417 (6.7) **CH_3CN** 285 (58.6), 304 (52.9), 323 (49.5), 422 (8.9) **Toluene**
4-Cl	275 (64.7), 293_{sh} (50.7), 320_{sh} (18.7), 339 (11.9) **CH_2Cl_2**
4-Br	275 (71.6), 295_{sh} (51.5), 320_{sh} (24.2), 340 (21.5), 395 (10.1) **CH_2Cl_2**
4-I	265 (44.3), 350 (10.2), 468 (12.8) **CH_2Cl_2**
5	287 (61.2), 320_{sh} (28.7), 403 (6.6) **CH_2Cl_2**

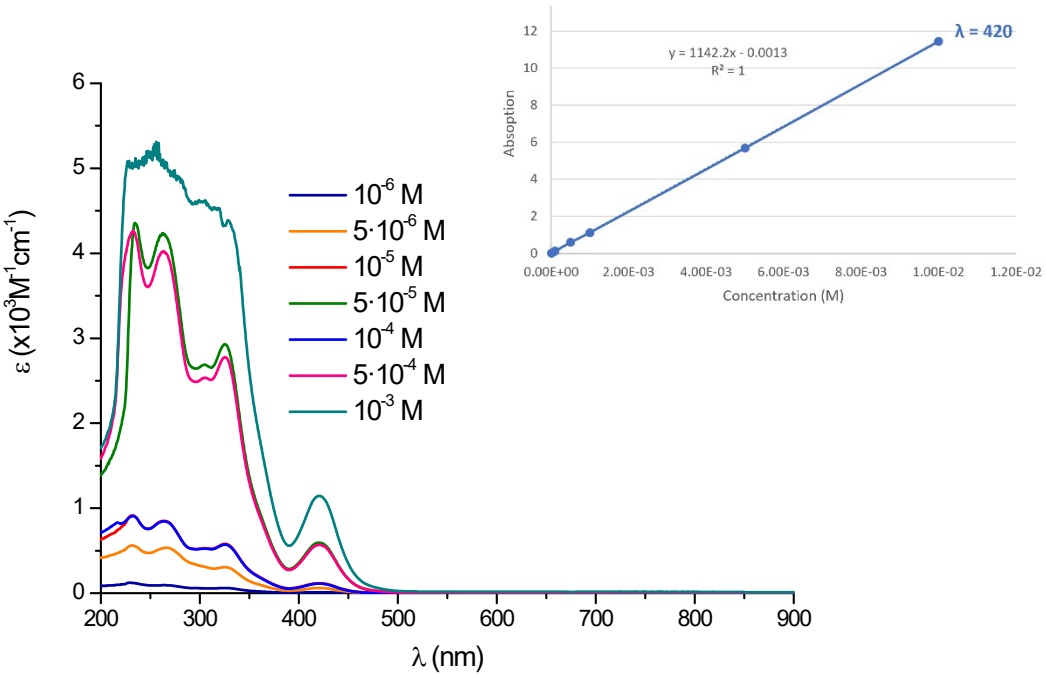

Figure S10. UV-Vis absorption spectra of **3** in CH_2Cl_2 at several concentrations at r.t. Inset: linear fit representations of the absorbances at 420 nm vs concentration.

Table S4. TD-DFT Vertical Excitations of Selected S_n excited states in the gas phase

Compound	λ[nm] (S_n)	o.s.	Transition (% contribution)*	Assignment
3	408.72 (S_1)	0.0792	HOMO → LUMO (91)	MMLCT
	373.01 (S_2)	0.0376	HOMO → L+1 (91)	MMLCT
4-Cl	563.16 (S_1)	0.0012	H-1 → LUMO (88)	L'MMCT / L'XCT
	532.75 (S_2)	0.0009	HOMO → LUMO (83)	L'MMCT / L'XCT
	460.19 (S_3)	0.0071	H-6 → LUMO (56), H-2 → LUMO (20)	LMMCT / L'MMCT/ XMMCT
	442.45 (S_4)	0.0000	H-3 → LUMO (45), H-5 → LUMO (21), H-9 → LUMO (20)	LMMCT / L'MMCT
	419.61 (S_5)	0.0134	H-3 → LUMO (21), H-2 → LUMO (20), H-6→ LUMO (15) H-5→ LUMO (13), H-9 → LUMO (5)	LMMCT / XMMCT
4-I	645.16 (S_1)	0.0008	H-1 → LUMO (96)	L'MMCT / L'LCT/ L'XCT
	618.62 (S_2)	0.0031	H-2 → LUMO (89)	L'MMCT / XMMCT
	591.78 (S_3)	0.0001	H-3 → LUMO (95)	L'MMCT/ XMMCT/L'LCT/XLCT
	590.27 (S_4)	0.0073	H-4 → LUMO (73), H-6 → LUMO (13), HOMO → LUMO (10)	XMMCT
	571.70 (S_5)	0.0003	H-5 → LUMO (96)	XMMCT / L'MMCT
	570.00 (S_6)	0.0200	H-6 → LUMO (58), H-4 → LUMO (23), HOMO → LUMO (14)	XMMCT / L'MMCT
	513.66 (S_7)	0.1333	HOMO → LUMO (36); H-9 → LUMO (36), H-6 → LUMO (18)	LMMCT / LXCT
5	521.36 (S_1)	0.0138	HOMO → LUMO (94)	L'MMCT/ L'RCT
	484.52 (S_2)	0.0417	H-1 → LUMO (94)	L'MMCT/ L'RCT
	426.20 (S_3)	0.0435	H-2 → LUMO (87)	LMMCT/ LRCT

*Transitions with contributions <5% are omitted

Table S5. TD-DFT Vertical Excitations of Selected S_n excited states in gas phase

MO	eV				Pt				C^C* (L)				N^N (L')				X (Cl, I) / R (Me)		
	3	**4-Cl**	**4-I**	**5**	**3**	**4-Cl**	**4-I**	**5**	**3**	**4-Cl**	**4-I**	**5**	**3**	**4-Cl**	**4-I**	**5**	**4-Cl**	**4-I**	**5**
L+1	-0.87				16				80				4						
L	-1.05	-2.37	-2.78	-4.56	16	56	46	47	80	13	10	27	4	4	3	6	27	40	20
H	-5.05	-5.67	-5.48	-7.95	81	4	15	10	10	2	13	4	9	87	21	86	7	51	0
H-1	-5.37	-5.68	-5.74	-8.04	23	8	7	6	4	2	2	18	73	88	58	76	1	33	0
H-2	-5.50	-5.98	-5.75	-8.31	9	13	2	5	20	58	11	80	71	3	36	15	25	52	0
H-3		-6.17	-5.87			5	5			94	3			0	20		1	72	
H-4		-6.35	-5.89			2	4			83	4			8	10		7	82	
H-5		-6.40	-5.95			4	5			1	3			61	25		34	67	
H-6		-6.41	-6.00			16	7			10	18			31	34		43	41	
H-9		-6.51	-6.45			7	14			2	64			60	13		31	9	

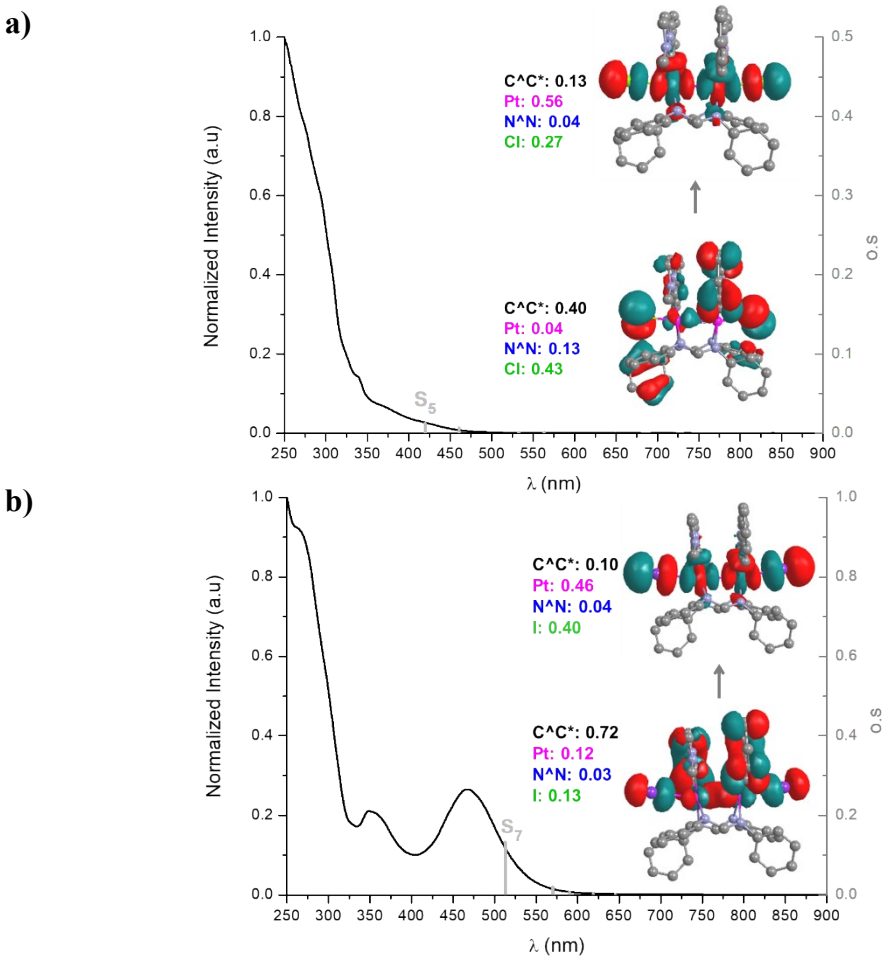

Figure S11. Normalized absorption spectra in solution, calculated S_n transitions in the gas phase (gray bar) for compounds **4-Cl** (a) and **4-I** (b). NTO analysis for the selected state; the calculated orbitals (isoval. 0.02) are depicted as a transition from hole (bottom) to particle (top).

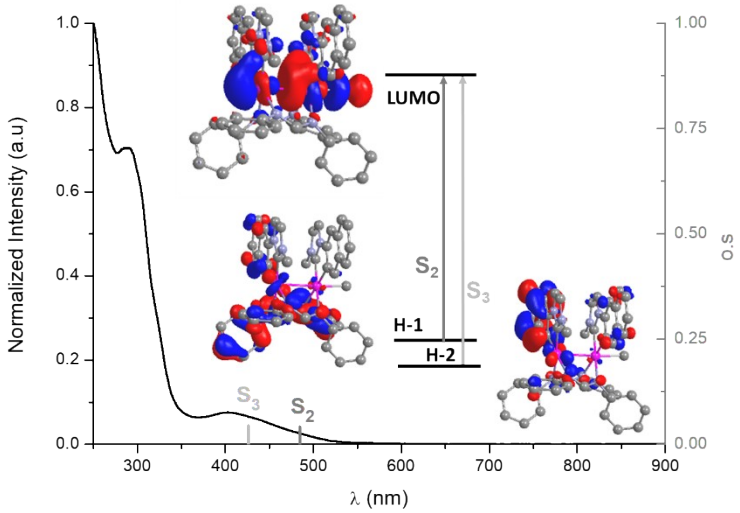

Figure S12. Normalized absorption spectra in solution, calculated S_n transitions (gray bar), and molecular orbital plots (isoval. 0.03) for compound **5**

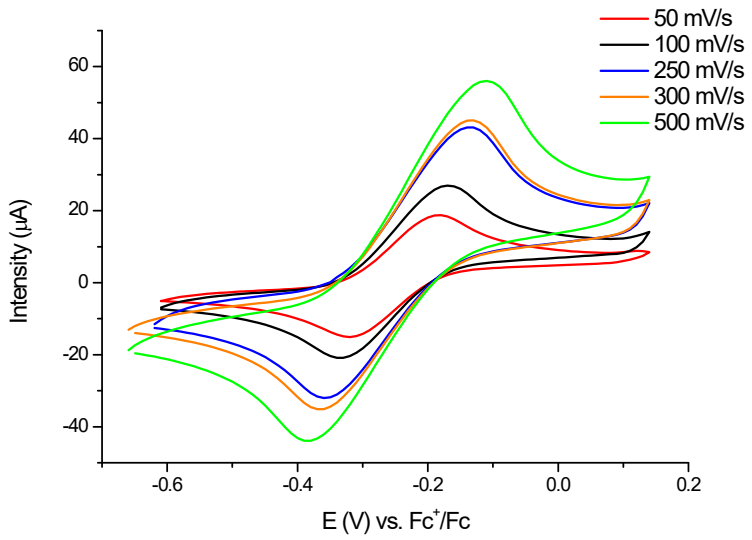

Figure S13. Cyclic voltammogram of **3** in CH_2Cl_2 at different scan rates

Table S6. Electrochemical data for **3** in CH_2Cl_2 at 100 mV/s.

Comp.	E_{ox} (V)	E_{red}(V)	ΔE_p(V)	E_{onset}(V)	E_{HOMO}(eV)	E_{LUMO}(eV)	Eg(eV)
3	-0.230	-0.329	0.99	-0.338	-4.762	-2.15	2.61

E_{HOMO} (eV) = – (E*onset ox* + 5.1) in the Fermi scale; E_{LUMO} (eV) = E_{HOMO} + Eg (eV); Eg = 1240 /$\lambda_{UV\text{-}VIS}$ [nm]

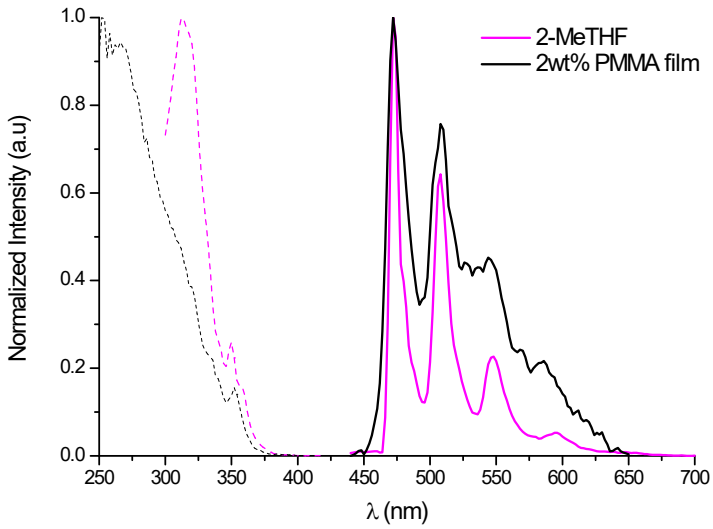

Figure S14: Normalized excitation (---) and emission (—) spectra of **2** in 2-MeTHF ($5 \cdot 10^{-5}$ M) at 77 K and in PMMA film

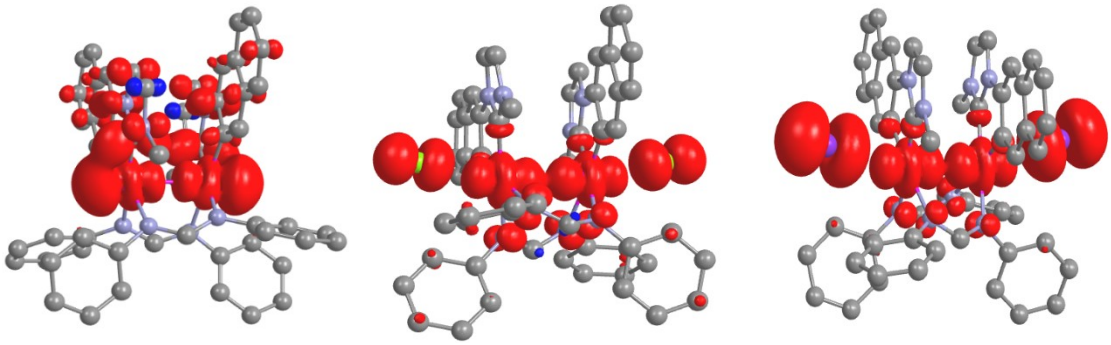

3 **4-Cl** **4-I**

1.18 0.82 0.00 **0.69 0.17 0.38 0.76** **0.56 0.14 0.20 1.10**

Figure S15. Spin-density distributions (**Pt C^C N^N X**; isovalue 0.002) calculated in gas phase for the T_1 states.

Table S7. Calculated bond parameters at the optimized geometries of the ground state (S_0) and the first triplet state (T_1).

	d Pt-Pt (Å) / Mayer BO	
Compound	**S_0**	**T_1**
3	2.993 / 0.09	2.761 / 0.59
4-Cl	2.687 / 0.69	2.947 / 0.31
4-I	2.735 / 0.61	2.931 / 0.21
5	2.805 / 0.39	*

*see computational methods section

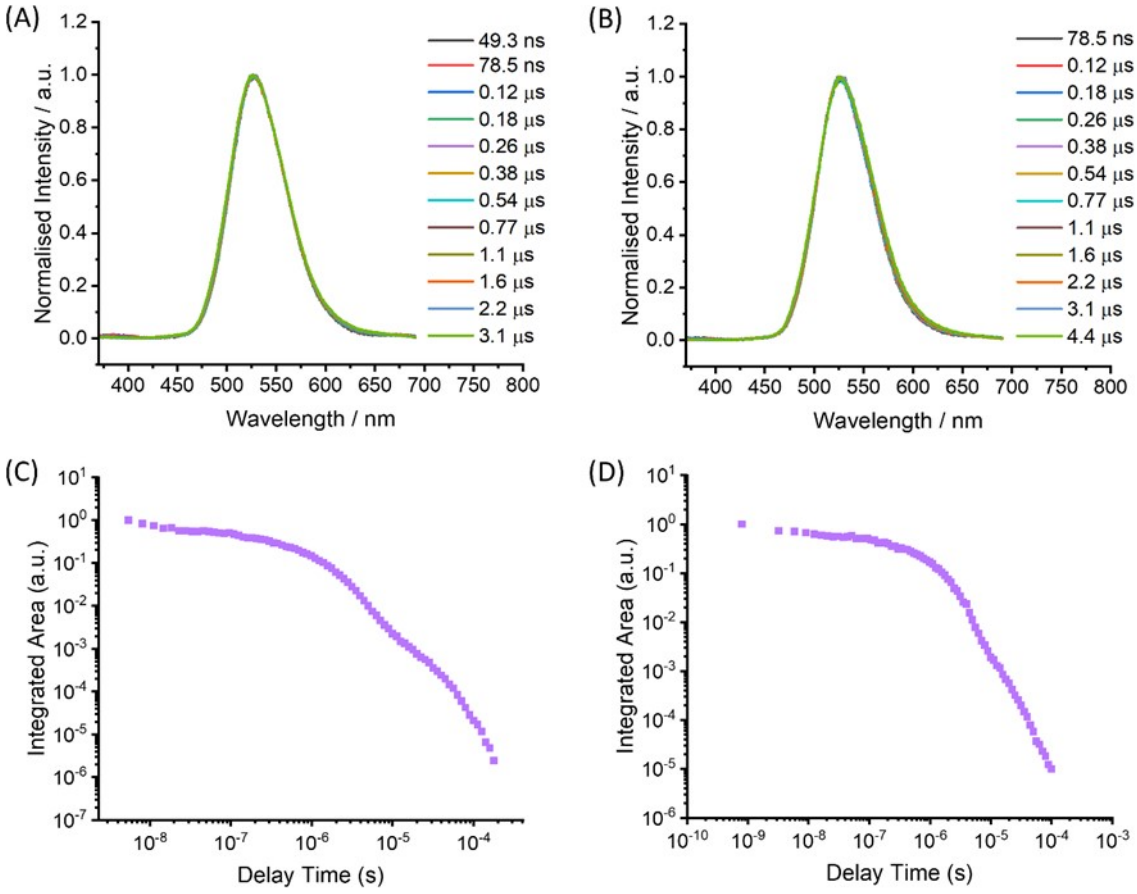

Figure S16. (A) Photoluminescence spectra for **3** in (A) 1.5wt% and (B) 1.5wt% CBP film measured at different delay times specified in the legend. Time resolved photoluminescence decay for the (C) 1.5wt% and (D) 1.5wt% CBP film measured at room temperature under vacuum**.**

4. OLEDs characterization

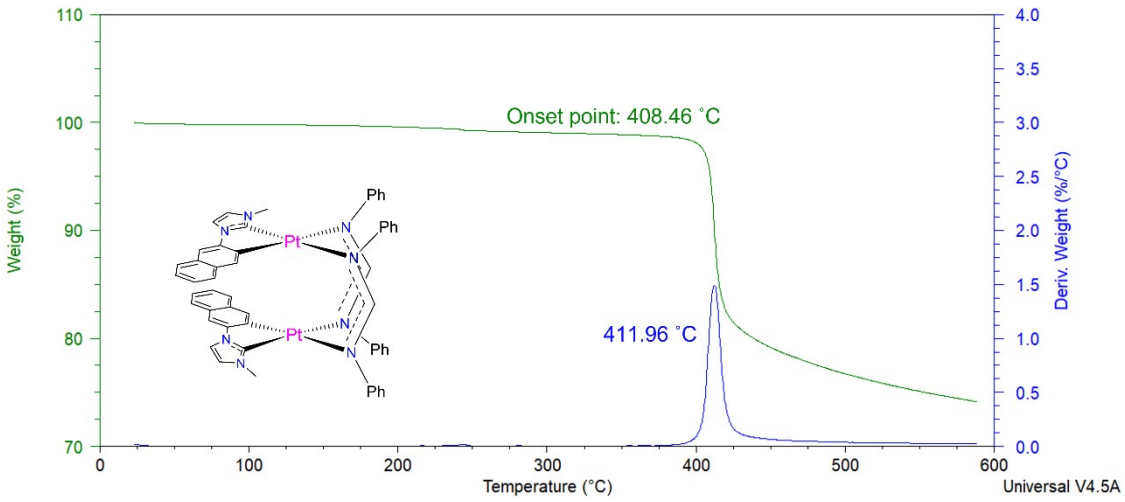

Figure S17. TGA recorded on heating at 10 °C min^{-1} under argon atmosphere (1 atm)

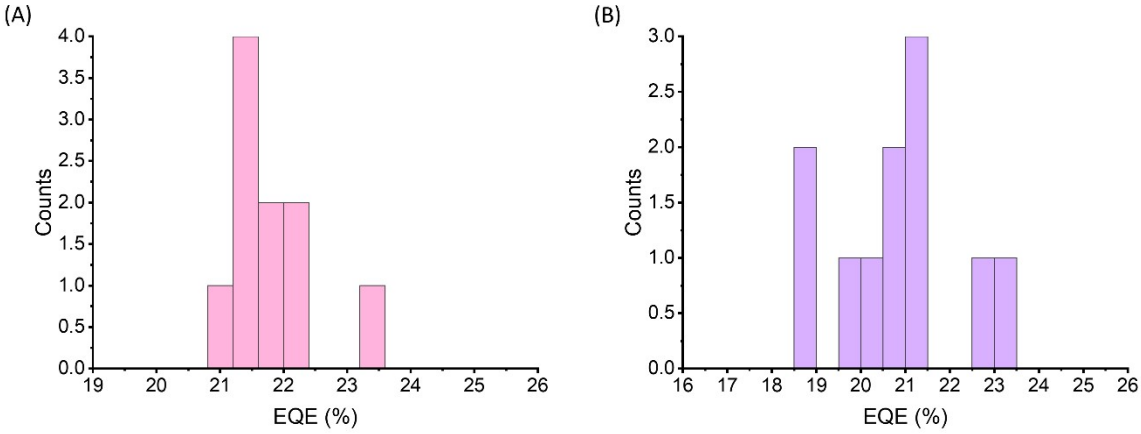

Figure S18. Histograms for the external quantum efficiency (EQE) of the individual pixels for the (A) 1.5% CBP and (B) 3% CBPOLED devices for complex **3**.

References

1. S. Fuertes, H. García, M. Perálvarez, W. Hertog, J. Carreras and V. Sicilia, Stepwise Strategy to Cyclometallated PtII Complexes with N-Heterocyclic Carbene Ligands: A Luminescence Study on New β-Diketonate Complexes, *Chem. - Eur. J.*, 2015, **21**, 1620-1631.
2. S. SAINT, Bruker Analytical X-ray Systems, Madison, WI, 2012.
3. L. J. Bourhis, O. V. Dolomanov, R. J. Gildea, J. A. K. Howard and H. Puschmann, The anatomy of a comprehensive constrained, restrained refinement program for the modern computing environment-Olex2 dissected, *Acta Crystallographica a-Foundation and Advances*, 2015, **71**, 59-75.
4. G. M. Sheldrick, Crystal structure refinement with SHELXL, *Acta Crystallogr. Sect. C*, 2015, **71**, 3-8.
5. M. J. Frisch, G. W. Trucks, H. B. Schlegel, G. E. Scuseria, M. A. Robb, J. R. Cheeseman, G. Scalmani, V. Barone, B. Mennucci, G. A. Petersson, H. Nakatsuji, M. Caricato, X. Li, H. P. Hratchian, A. F. Izmaylov, J. Bloino, G. Zheng, J. L. Sonnenberg, M. Hada, M. Ehara, K. Toyota, R. Fukuda, J. Hasegawa, M. Ishida, T. Nakajima, Y. Honda, O. Kitao, H. Nakai, T. Vreven, J. A. Montgomery Jr., J. E. Peralta, F. Ogliaro, M. J. Bearpark, J. Heyd, E. N. Brothers, K. N. Kudin, V. N. Staroverov, R. Kobayashi, J. Normand, K. Raghavachari, A. P. Rendell, J. C. Burant, S. S. Iyengar, J. Tomasi, M. Cossi, N. Rega, N. J. Millam, M. Klene, J. E. Knox, J. B. Cross, V. Bakken, C. Adamo, J. Jaramillo, R. Gomperts, R. E. Stratmann, O. Yazyev, A. J. Austin, R. Cammi, C. Pomelli, J. W. Ochterski, R. L. Martin, K. Morokuma, V. G. Zakrzewski, G. A. Voth, P. Salvador, J. J. Dannenberg, S. Dapprich, A. D. Daniels, Ö. Farkas, J. B. Foresman, J. V. Ortiz, J. Cioslowski and D. J. Fox, Gaussian 16*Journal*, 2016.
6. Y. Zhao and D. G. Truhlar, The M06 Suite of Density Functionals for Main Group Thermochemistry, Thermochemical Kinetics, Noncovalent Interactions, Excited States, and Transition Elements: two New Functionals and Systematic Testing of Four M06-Class Functionals and 12 Other Functionals, *Theor. Chem. Acc.*, 2008, **120**, 215-241.
7. S. Grimme, J. Antony, S. Ehrlich and H. Krieg, A Consistent and Accurate ab initio Parametrization of Density Functional Dispersion Correction (DFT-D) for the 94 Elements H-Pu, *J. Chem. Phys.*, 2010, **132**.
8. D. Andrae, U. Häußermann, M. Dolg, H. Stoll and H. Preuß, Energy-adjusted ab Initio Pseudopotentials for the Second and Third Row Transition Elements, *Theor. Chim. Acta*, 1990, **77**, 123-141.
9. R. Ditchfield, W. J. Hehre and J. A. Pople, Self-Consistent Molecular Orbital Methods. IX. An Extended Gaussian Type Basis for Molecular Orbital Studies of Organic Molecules, *J. Chem. Phys.*, 1971, **54**, 724-728.
10. P. C. Hariharan and J. A. Pople, The influence of polarization functions on molecular orbital hydrogenation energies, *Theor. Chim. Acta*, 1973, **28**, 213-222.
11. H. Leopold, M. Tenne, A. Tronnier, S. Metz, I. Muenster, G. Wagenblast and T. Strassner, Binuclear CC Cyclometalated Platinum(II) NHC Complexes with Bridging Amidinate Ligands, *Angew. Chem. Int. Ed.*, 2016, **55**, 15779-15782.
12. F. Wurl, S. Stipurin, J. I. Kollar and T. Strassner, Synthesis and Photophysical Properties of Monometallic C∧C* Platinum(II) Formamidinate Complexes using Sterically Demanding Ligands, *Angew. Chem. Int. Ed.*, 2023, **62**.
13. M. Xue, T. L. Lam, G. Cheng, W. Liu, K. H. Low, L. Du, S. Xu, F. F. Hung, D. L. Phillips and C. M. Che, Exceedingly Stable Luminescent Dinuclear Pt(II) Complexes with Ditopic Formamidinate Bridging Ligands for High-Performance Red and Deep-Red OLEDs with LT₉₇ up to 2446 h at 1000 cd m⁻², *Adv. Opt. Mater.*, 2022, **10**.
14. S. F. Wang, L.-W. Fu, Y.-C. Wei, S. Liu, J. Lin, G. Lee, P.-T. Chou, J. Huang, C.-I. Wu, Y. Yuan, C.-S. Lee and Y. Chi, Near-Infrared Emission Induced by Shortened Pt–Pt Contact:

Diplatinum(II) Complexes with Pyridyl Pyrimidinato Cyclometalates, *Inorg. Chem.*, 2019, **58**, 13892-13901.
15. S. Stipurin and T. Strassner, Phosphorescent Bimetallic CΛC Platinum(ii) Complexes with Bridging Substituted Diphenylformamidinates, *Chem. Eur. J.*, 2022, **28**.
16. L. Yuan, H. Yao, Y. Shen and Y. Zhang, A cyclometalated Pt(II)–Pt(II) clamshell dimer with a triplet emission at 887 nm, *Dalton Trans.*, 2024, **53**, 5125-5132.
17. H. Yao, L. Qiao, L. Yuan, X. Luan, Y. Shen, Y. Zhang, L. Zhou and H. Bian, Synthesis of phosphorescent syn, anti-isomeric clamshell platinum(ii) dimers for OLED applications, *J. Mater. Chem. C*, 2024, **12**, 4473-4483.
18. Z. Wang, L. Jiang, Z.-P. Liu, C. R. R. Gan, Z. L. Liu, X. H. Zhang, J. Zhao and T. S. A. Hor, Facile formation and redox of benzoxazole-2-thiolate-bridged dinuclear Pt(ii/iii) complexes, *Dalton Trans.*, 2012, **41**, 12568-12576.
19. V. Sicilia, J. Forniés, J. M. Casas, A. Martin, J. A. López, C. Larraz, P. Borja, C. Ovejero, D. Tordera and H. Bolink, Highly Luminescent Half-Lantern Cyclometalated Platinum(II) Complex: Synthesis, Structure, Luminescence Studies, and Reactivity, *Inorg. Chem.* , 2012, **51**, 3427-3435.
20. H. R. Shahsavari, E. Lalinde, M. T. Moreno, M. Niazi, S. H. Kazemi, S. Abedanzadeh, M. Barazandeh and M. R. Halvagar, Half-lantern cyclometalated Pt(II) and Pt(III) complexes with bridging heterocyclic thiolate ligands: synthesis, structural characterization, and electrochemical and photophysical properties, *New J. Chem.*, 2019, **43**, 7716-7724.
21. X. Wu, D.-G. Chen, D. Liu, S.-H. Liu, S.-W. Shen, C.-I. Wu, G. Xie, J. Zhou, Z.-X. Huang, C.-Y. Huang, S.-J. Su, W. Zhu and P.-T. Chou, Highly Emissive Dinuclear Platinum(III) Complexes, *J. Am. Chem.Soc.*, 2020, **142**, 7469-7479.
22. I. Melendo, S. Fuertes, A. Martín and V. Sicilia, NIR-II Emission from Cyclometalated Dinuclear Pt(III) Complexes, *Inorg. Chem.*, 2024, **63**, 5470-5480.
23. I. Melendo, P. Borja, S. Fuertes, A. Martín and V. Sicilia, Double-Decker Platinum Complexes: From Visible to NIR-II Luminescence, *Inorg. Chem.*, 2025, **64**, 17523-17532.
24. S. Fuertes, A. J. Chueca, M. Perálvarez, P. Borja, M. Torrell, J. Carreras and V. Sicilia, White Light Emission from Planar Remote Phosphor Based on NHC Cycloplatinated Complexes, *ACS App. Mat. Interfaces*, 2016, **8**, 16160-16169.
25. L. Arnal, S. Fuertes, A. Martín, M. Baya and V. Sicilia, A Cyclometalated N-Heterocyclic Carbene: The Wings of the First Pt2(II,II) Butterfly Oxidized by CHI3, *Chem. Eur. J.* , 2018, **24**, 18743-18748.
26. L. Arnal, D. Escudero, S. Fuertes, A. Martin and V. Sicilia, High-Valent Pyrazolate-Bridged Platinum Complexes: A Joint Experimental and Theoretical Study, *Inorg. Chem.*, 2022, **61**, 12559-12569.
27. V. Sicilia, L. Arnal, S. Fuertes, A. Martin and M. Baya, Metal-Metal Cooperation in the Oxidation of a Flapping Platinum Butterfly by Haloforms: Experimental and Theoretical Evidence, *Inorg. Chem.*, 2020, **59**, 12586-12594.
28. S. Fuertes, A. J. Chueca and V. Sicilia, Exploring the Transphobia Effect on Heteroleptic NHC Cycloplatinated Complexes, *Inorg. Chem.*, 2015, **54**, 9885-9895.